NASA CONTRACTOR REPORT

NASA CR-107

c.1

NASA CR-1072

PLASMA BOUNDARY INTERACTIONS - II

by S. Aisenberg, P. Hu, V. Rohatgi, and S. Ziering

Prepared by
SPACE SCIENCES INCORPORATED
Waltham, Mass.
for

NATIONAL AERONAUTICS AND SPACE ADMINISTRATION • WASHINGTON, D. C. • JUNE 1968

NASA CR-1072

PLASMA BOUNDARY INTERACTIONS - II

By S. Aisenberg, P. Hu, V. Rohatgi, and S. Ziering

Prepared under Contract No. NASw-1014 by
SPACE SCIENCES INCORPORATED
Waltham, Mass.

for

NATIONAL AERONAUTICS AND SPACE ADMINISTRATION

For sale by the Clearinghouse for Federal Scientific and Technical Information
Springfield, Virginia 22151 – CFSTI price $3.00

ABSTRACT

A study has been made of additional factors describing plasma-boundary interactions. The theoretical analysis of the sheath has been extended to include a transverse plasma flow outside the sheath region. The sheath model has been made more general, and also reveals the importance of the accommodation coefficients at the boundary surface. The presence of ionization and collisions in the sheath has also been studied theoretically. The interpretation of the experimentally observed threshold in the tangential electrode drag as a function of transverse magnetic field and of arc current has suggested the possibility of a threshold in the tangential accommodation coefficient. The threshold tangential energy appears to be proportional to the sputtering threshold and can be related to the threshold for displacement of surface atoms. The relationship between plasma phase velocity and particle velocity was studied and it was shown that there is not necessarily a simple connection: The related problem of arc retrograde motion (where plasma phase and particle motion have opposite signs) was studied and a simple model was proposed. It appears that the plasma propagates in the retrograde direction because of an increased net ion generation rate due to the inhibited diffusion loss of ions and electrons in the region of higher magnetic field. The importance of direct measurement of ion and atom velocity by means such as the Doppler shift is discussed.

CONTENTS

Section			Page
	ABSTRACT		iii
	ILLUSTRATIONS		vi
	TABLE OF TABLES		vii
	LIST OF SYMBOLS		ix
1	INTRODUCTION		1
2	THEORY		3
	2.1	Collisionless Plasma Sheath with Transverse Flow	3
	2.2	Collision and Ionization Effects in a Plasma Sheath	6
	2.3	Theory of Arc Propagation in Magnetic Fields	8
3	EXPERIMENTAL STUDIES		13
	3.1	Results of the Experiment	15
	3.2	Interpretation of Results	18
	3.3	Determination of Tangential Velocity	22
4	SUMMARY		27
	ACKNOWLEDGMENT		29
	REFERENCES		30
Appendix A	COLLISIONLESS PLASMA SHEATH WITH TRANSVERSE FLOW		A-1

ILLUSTRATIONS

Figure		Page
1	Schematic of Rotary Electrode Structure for the Measurement of Tangential, Anode, and Cathode Electrode Forces	14
2	Drag Force on Electrodes of a JxB Arc as a Function of Magnetic Field	16
3	Dependence of Cathode Drag Force on the Arc Current	17
4	Electrode Geometry and Fiber Optic Arrangement for the Measurement of Particle Velocity by the Doppler Shift Method	25

TABLE OF TABLES

Table		Page
1	Drag Force and Sputtering Thresholds	21

LIST OF SYMBOLS

Symbol	Definition
a	Normalized potential difference across sheath
B	Magnetic field
B_θ	Self magnetic field of arc
c	Velocity of light
D_a	Ambipolar diffusion coefficient
D_{ab}	Ambipolar diffusion coefficient in magnetic field
G	Rate of production of ions and electrons
I	Arc current
J	Current density
n	Particle density
p_c	Critical pressure to stop retrograde motion
t	Time variable
T	Temperature
v	Particle velocity
v^+	Transverse velocity component of ions in sheath
V	Voltage
V^+	Transverse velocity component of ions at sheath edge
λ	Wave length
μ_{io} μ_{eo}	Ion and electron mobilities in zero B field

1. INTRODUCTION

This report covers the second phase of a research program under NASA sponsorship entitled "Electrode Effects in JxB Accelerators" during the period August 1, 1966 to July 31, 1967. Much of the research carried on during this latter phase continues and extends in a logical fashion the work started in the earlier phase. In order to emphasize in this report mainly the new and significant aspects of work previously not fully documented, frequent reference will be made to a previous summary report[1], to a recently issued NASA Contractor Report[2] highlighting some of our more significant results and conclusions, and to various scientific publications generated under the program[3 - 11]. Thus it is hoped that the reader will avail himself of the above cited references for detailed background information, and regard this specific report as an integral part in conjunction with previous reports (particularly Ref. 2). The theoretical effort will be summarized in Section 2 which is divided into three subsections by subject matter. Section 3 discusses the experimental measurement of plasma electrode drag and the implications relative to ion current partitioning and the momentum accommodation coefficients. Also described is the experimental effort on velocity measurements by Doppler Shift techniques.

Following these specific discussions, a summary of the status of the overall program at Space Sciences Incorporated is presented in Section 4. A complete report entitled "Collisionless Plasma Sheath with Transverse Flow," of which a condensed version will be published in the Physics of Fluids, is included as an Appendix.

The following is a composite list of all reports, publications, and presentations that have resulted from this program in the last year.

THE FOLLOWING REPORTS AND PUBLICATIONS HAVE RESULTED FROM THIS PROGRAM IN THE LAST YEAR AND SHOULD BE CONSULTED FOR ADDITIONAL DETAILS

Reports, Publications, and Presentations

P. N. Hu and S. Ziering, "Collisionless Plasma Sheath with Transverse Flow." Presented at the Eighth Annual Meeting of the Plasma Physics Division, American Physical Society, Boston, Mass., Nov. 1966.

V. Rohatgi and S. Aisenberg, "Tangential Momentum Transfer to the Electrodes of a Magnetically Accelerated Arc." Presented at the Eighth Annual Meeting of the Plasma Physics Division, American Physical Society, Boston, Mass., Nov. 1966.

S. Aisenberg and V. Rohatgi, "A Study of Electron Emission Processes at Arc Cathodes." Presented at the Eighth Annual Meeting of the Plasma Physics Division, American Physical Society, Boston, Mass., Nov. 1966.

S. Aisenberg, "Plasma Propagation Theory of Arc Retrograde Motion," Presented at the Eighth Symposium on the Engineering Aspects of MHD, March 1967.

V. Rohatgi and S. Aisenberg, "Ion Drag and Current Partitioning at the Cathode of a Plasma Accelerator." Presented at the AIAA Joint Electric Propulsion and Plasma Dynamics Conference, Colorado (September 1967).

P. N. Hu and S. Ziering, "Collisionless Plasma Sheath with Transverse Flow," Tech. Rept. 406-4, SSI, 1967. Also to be published in Physics of Fluids in a condensed form.

P. N. Hu and S. Ziering, "Collision and Ionization Effects in a Plasma Sheath," Tech. Rept. 406-13, SSI 1967. To be published in the Journal of Plasma Physics.

S. Aisenberg, P. N. Hu, V. Rohatgi, and S. Ziering, "Plasma-Boundary Interactions," NASA Contractor Report, NASA CR-868, Washington, D.C. August, 1967.

2. THEORY

In the previous reporting period (see Ref. 2), a microscopic kinetic theory approach to the problem of the plasma sheath was formulated. In order to compare this approach with the more standard and restrictive theories (e.g., Bohm's Sheath Criterion) a normal incident flow on the electrodes was assumed initially. The physically more meaningful and interesting problems,however, require that the plasma flows parallel to the electrode. Thus, during the latest performance period, the sheath problem analysis by kinetic theory was extended so as to include a transverse flow; this is discussed in Section 2.1. Both of the above mentioned sheath treatments pertain to the collisionless domain and therefore are only valid within, at most, a mean free path away from the physical boundary. Therefore, as a next logical step in our attempt to bridge the understanding between collisionless (sheath) and collision dominated (continuum) theories, SSI has included both collisions and ionizations in the kinetic theory description by utilizing the previously established model equation for ionization. This is summarized in Section 2.2 below. In Section 2.3 a discussion of the problem of plasma arc propagation in a transverse magnetic field, and in particular, an analysis of the process of retrograde arc motion is briefly presented.

2.1 Collisionless Plasma Sheath With Transverse Flow

The previously developed sheath model (Ref. 3 and 4) has been extended to include the more realistic effects of a transverse bulk flow of the plasma outside the sheath region. As in the previous sheath model, very general microscopic boundary conditions are incorporated at the electrode to take into account any possible plasma-boundary interactions. The transverse flow of the plasma is represented by assuming displaced Maxwellian distribution functions for particles coming from the sheath edge.

To this end a detailed analysis has been carried out in Ref. 4 (included as an Appendix). It has been found that any plasma property that does not involve the velocity moment of the distribution functions in the transverse direction remains unchanged and is the same as evaluated in Ref. (3). Thus, many of the physical quantities such as potential profile, charge densities, sheath thickness and ion current are independent of the transverse flow of the plasma. General expressions for those plasma properties that have been altered because of the inclusion of the transverse flow such as electron and ion drag forces and heat flows have been derived in detail in Ref.(4). As shown in Ref.(3), a simple analytic solution can be obtained for a special case where the temperatures of the electrons, the ions, and the electrodes are the same. The transverse ion and electron velocities, ion temperature and the potential profile for this special case are shown in Figures 1 through 4 in the Appendix. In the more general case where the temperatures are not the same, a simple numerical integration will yield these profiles. A condensed version of Ref. 4 has been accepted for publication in the Physics of Fluids.

From the figures we conclude that the transverse ion velocity at the cathode decreases rapidly with the increase of the potential difference across the sheath. Physically, this can be traced to the trapped ions near the cathode which are originated by diffuse reflections and do not carry any transverse momentum. As the potential difference increases, more ions are trapped and the transverse ion velocity at the cathode therefore diminishes. In comparison with the potential profile, we observe that the transverse ion velocity changes rather slowly with distance. Particularly, for large values of the potential difference (a), the maximum change of the ion velocity (v^+) occurs quite a distance away from the electrode. For instance, at a distance of a Debye length from the electrode, the potential drop has reached 84% of its total value across the sheath for a = 10, but the transverse ion velocity has only reached 8% of its value at the sheath edge. Even at a distance of 5 Debye lengths, v^+/V^+ is only about 82%. This indicates that the accelerated particles begin to adjust their transverse velocities quite far away from the electrode as compared with the potential changes for high potential differences across the sheath. Further examination shows that this

result is true not only for the present special case but also for the general case as can be seen from the expressions for the ion mass flow and density in Ref.(4). The transverse velocity profile of the ions is therefore an important effect to be taken into account in related practical problems.

The ion velocity slip can be calculated as

$$[V^+ - v^+(0)]/V^+ = \text{erf}(a)^{1/2} \qquad (1)$$

which increases monotonically with a.

Although the interpretation of many results depends on the plasma and surface (electrode) parameters to be specified, some general conclusions can be drawn as follows:

1. The transverse velocity of accelerated particles in the sheath varies rather slowly away from the electrode in comparison with the potential. Particularly, for high potential differences across the sheath, the maximum change of the transverse velocity for the accelerated particles occurs at a distance several Debye lengths from the electrode while the maximum change of the potential always occurs at the electrode. In other words, the effect of the electrode on the transverse velocity of accelerated particles may extend well beyond the distance of the sheath thickness, defined in the usual sense,for high potential difference across the sheath.

2. The drag force exerted on the electrode by accelerating particles is directly proportional to the transverse velocity at the sheath edge but is independent of the potential

difference across the sheath. On the other hand, the drag force due to repelled particles decreases rapidly with increasing potential differences across the sheath as one would intuitively expect.

The results and expressions obtained here are readily applicable to related problems such as the interaction of a solid body with a moving collisionless plasma.

2.2 Collision and Ionization Effects in a Plasma Sheath

In the study of a plasma sheath near an electrode or a physical boundary, the plasma in the sheath is usually considered collisionless when the mean free path is large compared with the Debye length and is considered collision dominated when the mean free path is small. Mathematically, the collisionless problem has been treated in complete generality and has been analyzed in terms of the electrode and plasma parameters to be specified (Section 2.1). However, many other phases of the physical problem remain to be explored. An important one is the region outside the collisionless sheath about a mean free path away from the cathode where the neutral particles emitted from the electrode are ionized again through collisions. In this region, collisional effects and ionization effects are equally important.

The most important application of the collisionless theory developed at SSI under the program is in the utilization of the results obtained for subsequent extension to the continuum domain. Except for possible numerical work, it is doubtful whether analytic results uniformly valid in the sheath and the collision domains can be obtained, because of the complexity. It is, therefore, suggested that the above rigorous sheath analysis can be used to provide the proper boundary conditions for a continuum approach extending beyond the sheath domain. Thus, our attention subsequent to the collisionless analysis emphasized the

transition domain. In the transition domain that spans these two limits, the analysis of the plasma sheath is characterized by all the difficulties encountered for neutral gases and is, in addition, complicated by the coupling between charged particles, ionization, neutralization, emission and absorption of particles at the physical boundaries. For practical considerations and mathematical tractability, we examine the approach from the collisionless to collisional theories with due regard to the general microscopic boundary conditions at the physical surface.

Because of the singular behaviour of the differential operator in the Boltzmann equation for particles that have vanishing velocity components normal to the physical boundary surface, it is well known that the dominant correction term to the collisionless solution for neutral gases with finite collision cross sections is proportional to $(\ell n\ K)/K$ in one-dimensional problems, where K is the Knudsen number defined as the ratio of the mean free path to the characteristic length of the problem. In a plasma of multiple components, the singular behaviour of the differential operator occurs in the Boltzmann equation for each component and the dominant collisional correction term in the near collisionless domain is therefore more complicated.

Another important phenomenon in a plasma sheath is the ionization process taking place near a cathode. The neutralized ions, reflected from the electrode as neutral particles, are eventually ionized again through collisions. The electron and ion currents are therefore not conserved because of the new electrons and ions generated in the ionization process. Furthermore, ionizing particles are at different energy levels before and after collisions and therefore can only be described through the change of their distribution functions.

To incorporate a kinetic description of the ionization process as well as the collision process in the study of a plasma sheath, the previously developed kinetic model (Ref. 5) is used. To reveal the contribution from the singular behaviour of the differential operators, a system of integral equations is formulated and the system is solved to the first order by an iteration method, starting

with a sheath solution in the collisionless limit as the zero order.

A thorough study of the problem based on this approach is carried out in Ref. (6) which will be published in the Journal of Plasma Physics. The collision effects with or without an electric field and the ionization effects on the densities and currents of electrons and ions as well as of neutrals are obtained. The results are discussed extensively for various cases.

There are many collisionless sheath models existing in the literature, including the one recently developed at SSI (Refs. (2) through (4). However, the analysis made in Ref. (6) is quite general, without being restricted to any specific sheath model and consequently the results as well as the discussions can be applied to any sheath models.

2.3 Theory of Arc Propagation in Magnetic Fields

As part of the interpretation of the plasma-electrode interactions, it was necessary to study the relationship between the plasma arc motion and the plasma particle motion. The actual interactions between the plasma and the electrodes occur through the atoms, ions, and electrons that actually strike the electrodes. Thus it is important to be able to specify or measure the particle velocities relative to the electrode surfaces. A more readily measured quantity is the velocity of the plasma arc itself. In order to use the plasma phase velocity, it is necessary to determine if there is a definite relationship between the plasma particle velocity and the plasma phase velocity. The results of the analysis of the problem showed that the plasma phase velocity is related to the rate of growth of plasma density and can not be readily used to measure the ion and atom tangential velocity.

The most direct proof of the difference between the phase and particle velocity is the well documented observation of retrograde arc motion at low presusres, where the plasma itself moves opposite to the normal motion of the charged particles. Thus, a study was made of the physical process involved

in arc retrograde motion. What appears to be a novel and satisfactory model, was developed and presented.[10] A brief outline of the plasma propagation theory of arc retrograde motion is presented in this section. This analysis should also lead to insight into the basic mechanisms of plasma propagation in a magnetic field, and should also indicate the relationship between electrode emission and plasma propagation.

The problem of retrograde arc motion in a transverse magnetic field will be discussed and a model will be proposed both to explain and predict many features of the retrograde motion.

Essentially, the concept of retrograde motion corresponds to the observation that an electric arc in an external magnetic field B will move in a direction perpendicular to both the current and the magnetic field. The motion of the arc is expected in view of the Lorentz force that acts upon a charged particle moving in a magnetic field. However, it is observed that under low-pressure conditions the arc moves in the direction opposite to that expected from the Lorentz forces. The arc motion in this case is called retrograde motion, and cannot be explained in terms of the opposite charges or opposite velocities of the positive ions and electrons.

If one is to feel that the plasma arc is understood, it is necessary to explain the phenomena of retrograde arc motion. Retrograde arc motion has been studied as far back as 1903[12] and by many subsequent researchers[13], but no really satisfactory explanation has been presented.

A model will be described here to explain the retrograde motion in terms of the plasma growth into regions where the magnetic field is larger. Thus the retrograde arc motion can be described as a process similar to phase velocity rather than actual retrograde particle velocity. The essential feature of this model for retrograde motion is that the diffusion and mobility loss of electrons and ions (ambipolar diffusion) is reduced by the presence of large magnetic fields. On the retrograde side of the arc, the self-magnetic field is in the same direction as the external field and is in the opposite direction in the Lorentz

side of the arc. The Lorentz force model predicts that the arc will move into regions where the magnetic field is weakest. (This can also be seen on the basis of the elastic magnetic flux model). The plasma growth model on the other hand predicts that the arc will grow in the direction where the magnetic field is largest; this prediction is in agreement with the observations of retrograde motion. This model was developed during a research program on electrode effects in JxB accelerators[1] and was also later used in a program studying electron-emission processes for a mercury arc cathode[14].

It is possible to describe mathematically the retrograde propagation process in order to predict the general dependence upon the arc parameters. For the plasma positive column, the time rate of change of electron (and ion density) n_e is given by,

$$\frac{dn_e}{dt} = G\,(n_e, T_e, B) - \text{div}\,(D_a\ \text{grad}\ n_e) \qquad (2)$$

where the generation term $G\,(n_e, T_e, B)$ is the rate of production of ions and electrons (as a function of electron density, electron temperature, and of magnetic field) and where the last term describes the loss of ions by ambipolar diffusion. The ambipolar diffusion coefficient D_a corresponds to the radial particle flow of ions and electrons.

The presence of a strong transverse magnetic field will change the mobility and diffusion coefficients[15] so that the ambipolar diffusion coefficient is D_{ab} as modified by a magnetic field B is,

$$D_{ab} = D_{ao}\,\frac{1}{1 + \mu_{io}\,\mu_{eo}\,B^2} \qquad (3)$$

where D_{ao} is the ambipolar diffusion coefficient in the absence of a magnetic field, and the terms μ_{io}, μ_{eo} correspond to the zero field values of the ion and electron mobility respectively.

The magnetic field term B in D_{ab} corresponds to the magnitude of the vector sum of the external field and the self-magnetic field B_θ of the arc. In the region where the two B fields are in the same direction they will add and the magnitude of B is larger so that D_a is smaller. The net rate of electron production dn_e/dt becomes more positive when the ambipolar loss becomes smaller so that the rate of electron production will be larger on the retrograde side and the arc will grow or propagate on the retrograde side. The reverse is true on the "Lorentz" side of the arc where the arc will decay. In general, therefore, for those regions where the total B (transverse) is larger,the ambipolar diffusion loss term is smaller and the arc will increase in those high B-field regions. At higher pressures, the dependence of D_a upon B is smaller because of reduced μ_{io} and μ_{eo}. The retrograde velocity is expected to increase with the plasma growth rate. Kesaev[16] uses a maximum field concept where the cathode spot on mercury will move in the direction of the largest increase in magnetic field, but he does not appear to specify the mechanisms involved.

Ecker and Müller[17] have presented an interesting theory to explain the retrograde motion. In their theory, the tilting of the ion beam flowing to the cathode is primarily responsible for the retrograde motion. Some of the aspects of retrograde motion, however, cannot be readily predicted by their theory.

The concept of retrograde motion due to plasma growth, however, can be used to predict many of the observed features of retrograde motion. Some of the predictions of the plasma-growth model are discussed briefly.

1. Retrograde motion should appear with all cathode materials, and has been reported for various solid metal and liquid cathodes[13] as well as for the thermionic cathode[18].

2. Retrograde motion has been reported for the anode spot[19] which is in agreement with the plasma-propagation model. (This observation is difficult to reconcile with the "ion-stream" model of Ecker and Müller because there is no ion stream at the anode.)

3. The retrograde velocity decreases as the gas pressure increases[13,20] and can be explained by the decrease of ion generation resulting from the reduction of electron temperature. Also, an increase of pressure implies an increase of ion and electron density together with an increased time to form the propagating plasma and thus a reduced retrograde velocity. The dependence of D_{ab} upon B is also reduced at large pressure.

4. The retrograde velocity increases with external B[20] and can be explained by a decrease of D_{ab}.

5. Retrograde velocity increases with current I but not very rapidly. This is probably due to a small variation of B_θ with I.

6. The critical pressure p_c required to stop retrograde motion is reported to increase with the ionization potential of the gas[21]. This interesting observation suggests that the retrograde motion is related to the ionization properties and the propagation of the plasma mode rather than to the actual transport of charged particles.

7. Windmill experiments show that the gas motion is in the correct Lorentz direction[22,23]. This is in agreement with the arc propagation theory.

It thus appears that many of the features of retrograde motion (as well as the actual direction) can be explained by the model of plasma propagation growth in the direction of large total magnetic fields where the ambipolar diffusion is reduced.

3. EXPERIMENTAL STUDIES

As part of the study of the physical phenomena of plasma boundary interactions in JxB accelerators, tangential drag forces on the electrodes were measured earlier in this program[2]. More extensive measurements have been made for other electrodes and arc gases. Additional interpretation of the results have resulted in further information about the plasma-electrode processes. It is shown from these experiments that a considerable fraction of the driving JxB force is transferred to the solid boundaries and can account for the excessive electrode damage and the low efficiences of plasma accelerators. The drag forces are related to the processes of momentum transfer to the electrodes by various charged and neutral particles. The positive ion current contribution is indicated by higher drag force at the cathode. From this study it is estimated that at the cathode about 10 percent of the current is carried by the ions. A threshold in the drag force is observed at lower JxB values. The significance of the drag threshold was investigated. The present data suggests a relation between the drag and the sputtering thresholds.

Figure 1 illustrates the apparatus used for the measurement of tangential electrode forces. The rotary electrode was made of molybdenum (and also of copper) rod about 10 cm long with a 2 cm diameter. The active electrode however, was only 2 cm in diameter and 1 cm long. The arc current to this electrode was fed through a liquid mercury pool. A thick layer of low vapor pressure silicone oil was provided on the mercury surface to suppress the Hg vapor contamination in the arc plasma. To reduce the homopolar and electromagnetic forces in the liquid pool commutator, the contact was designed and insulated (Figure 1, Detail A) so as to force the current to flow parallel to the magnetic field in the Hg pool. Also, the current into the electrode was injected at the same radial point at which it left the electrode thus minimizing the homopolar forces.

The fixed electrode of the plasma generator consisted of a water cooled copper ring, 1 cm thick and about 9 cm in diameter with a 4 cm diameter hole in the center. This was located symmetrically around the rotary electrode so that the arc ran radially in a gap 1 cm long and 1 cm wide. By using ring

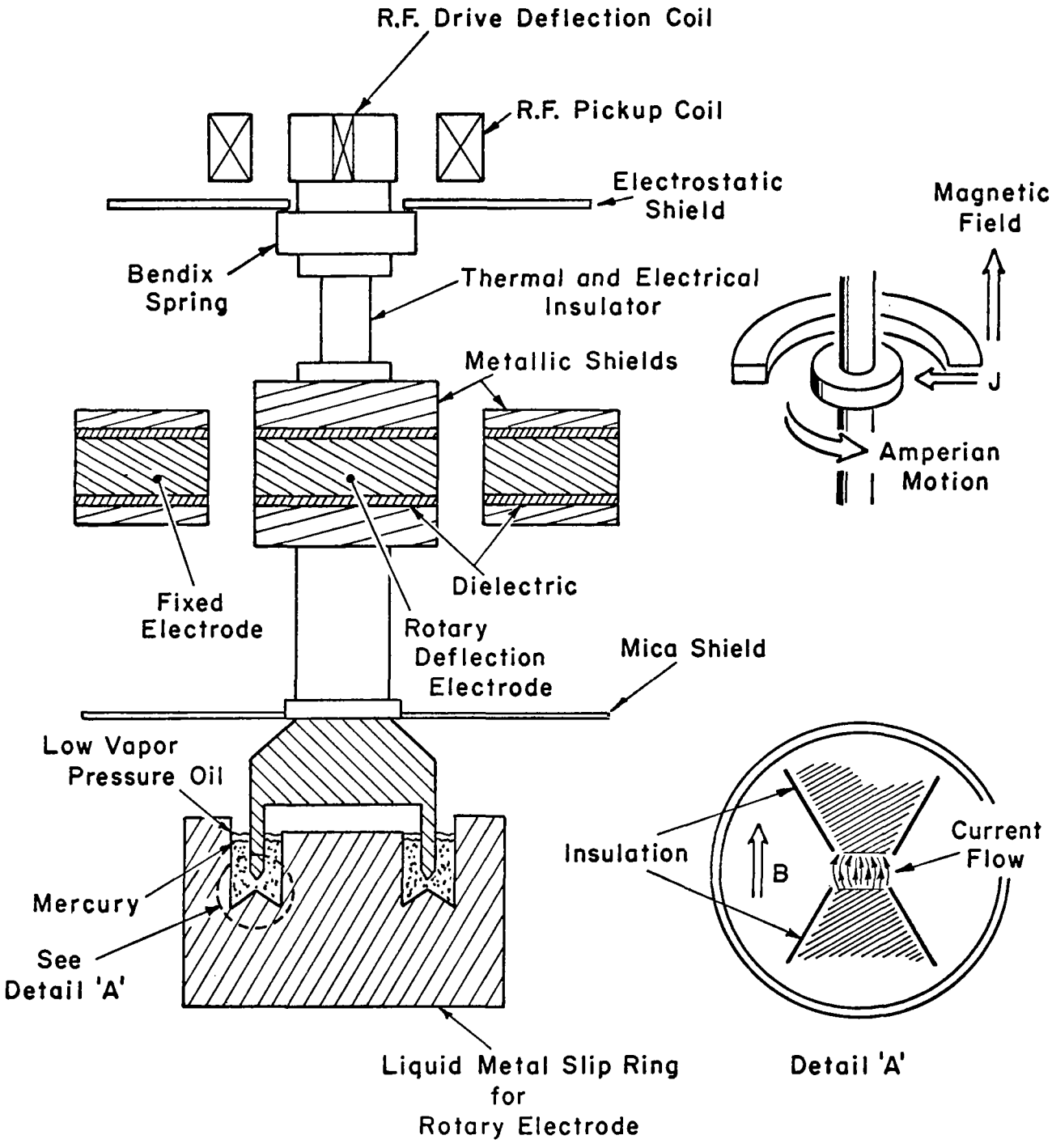

FIGURE 1.

SCHEMATIC OF ROTARY ELECTRODE STRUCTURE FOR THE MEASUREMENT OF TANGENTIAL, ANODE, AND CATHODE ELECTRODE FORCES.

electrodes with different inner diameters, the length of the plasma could be varied conveniently. Provision was made so that the center rotary electrode could be used as a cathode or as an anode.

A magnetic field parallel to the axis of rotation was generated with a water-cooled conventional air core electromagnet, located outside the vacuum chamber. A Helmholtz coil structure was adopted to create a uniform field in the test region.

The rotary structure was supported on a Bendix torsion spring, so that the tangential force on the electrode was measured in terms of the spring deflection. The small angular displacements of the spring were detected by a multiple coil rf transducer. The torque balance was calibrated with known weights and lever arms each time the apparatus was assembled. The observed good ringing characteristics show low system damping and the absence of hysteresis due to friction.

3.1 Results of the Experiment

The drag forces on cathode and anode electrodes were measured by operating the central electrode as cathode and anode respectively. Some of the preliminary studies of the tangential forces on a molybdenum electrode in argon only have been described earlier[24]. In Figures 2 and 3 are illustrated the results of measurements of the drag forces on copper and molybdenum electrodes in argon plasmas. These measurements indicate that for these electrode materials and these gases:

1. The drag forces at both electrodes were in Amperian direction and changed sign when the B field was reversed.

2. The anode drag force was smaller than the cathode drag force, thus indicating that the ion current contribution to cathode drag was significant.

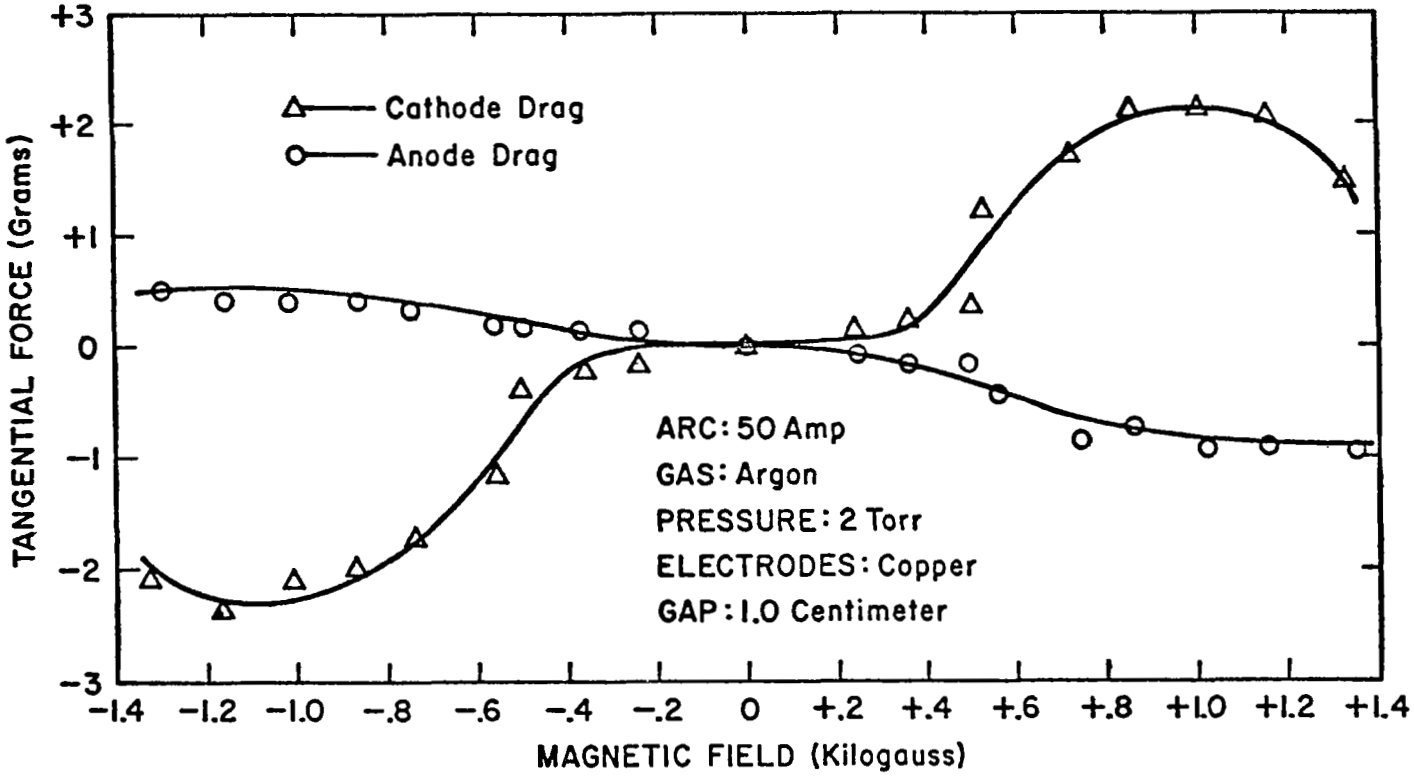

FIGURE 2.

DRAG FORCE ON ELECTRODES OF A JxB ARC
AS A FUNCTION OF MAGNETIC FIELD.

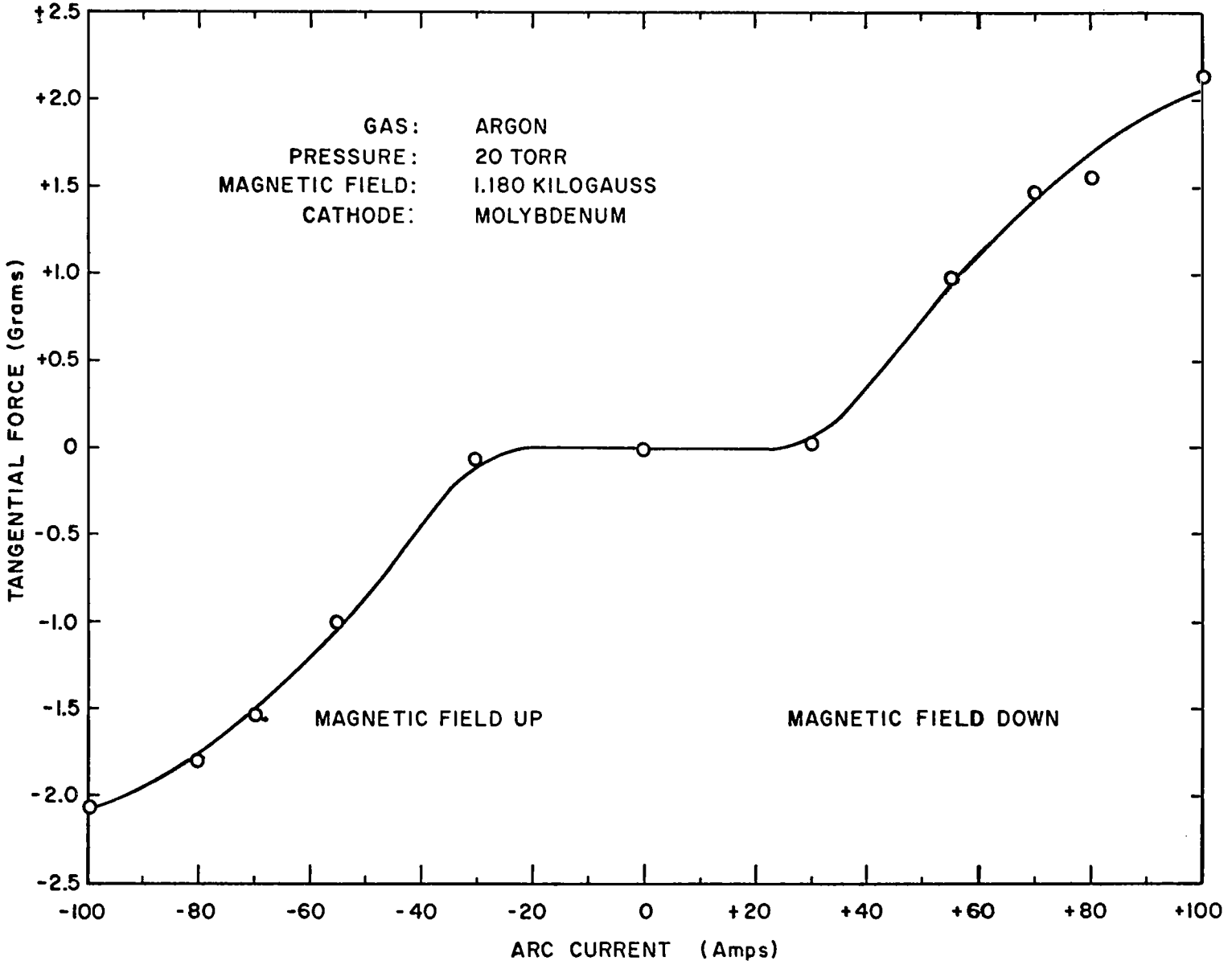

FIGURE 3.

DEPENDENCE OF CATHODE DRAG FORCE ON THE ARC CURRENT.

3. The drag force was a complex function of the magnetic field showing a threshold effect at lower fields and a saturation effect at higher B fields.

4. The drag force at the cathode shows a threshold effect also with respect to arc current.

3.2 Interpretation of Results

The experiments reported here reveal several interesting processes involved in the plasma-surface interaction. The measurements of the tangential forces indicate that a significant fraction of the JxB plasma driving force appears at the electrodes. As much as 20 to 30 percent of the plasma acceleration force is recorded at the cathode while the anode takes up another 10 to 15 percent of the JxB force. Thus, in general for this accelerator structure about 30 to 45 percent of the total driving force is transferred to the arc electrodes. Higher forces at the cathode show an appreciable contribution due to ion current drag[2,8,11].

In order to deduce the cathode drag due to positive ions it was necessary to compare the drag at the anode and cathode and to ascribe the difference to the ion current which flows to the cathode only. An important assumption implicitly made, is that the drag due to the neutral gas in the arc plasma is the same at the anode and at the cathode. Because of the different ion and electron sheaths at the cathode and anode respectively, it is possible that the neutral gas drag is different at each electrode; it is expected, however, that the difference will be small. A detailed analysis of this effect is recommended.

The tangential drag due to neutral gas atoms at the electrodes is determined by the product of the neutral gas density, the tangential gas velocity, and the neutral particle velocity to the electrodes. These neutral particles are not directly influenced by the electric fields so that it is expected that the neutral gas drag at the two electrodes will be essentially the same. The neutral gas density should be the same at the cathode and anode sheaths. The arc tangential

velocity should also be the same at both electrodes. Because of the positive ions flowing toward the cathode, it is possible that (due to the momentum transferred in ion-atom collisions) the neutrals can be driven towards the cathode at a rate larger than the random gas velocity. For low ion current densities in the cathode sheath, it is expected that the gas atoms will experience very few ion collisions on the way to the cathode. A more detailed calculation of this effect at the cathode and anode is being performed for further study of this problem.

The ion current drag deduced from the difference between the cathode and anode drag is about 0.5 of the cathode drag so that this determination is relatively free from magnified errors due to taking small differences of larger numbers.

The effect on the drag force of total gas motion (in the chamber) was investigated by putting axial shields around the plasma acceleration channel. Within the accuracy of this test, the data with and without the shields demonstrated that the electrode force was unaffected by the modification in the axial gas flow away from the electrodes. It may thus be concluded that the forces transferred to the electrodes were predominantly related to the interaction of the arc root at the electrodes, and not to the mass motion of the gas.

The presence of tangential electrode (and boundary) friction forces is expected for a hot plasma flowing in a channel when one considers that some of the tangential momentum is transferred each time an ion, electron, or gas atom collides with the surface. It has been suggested by Thom, Norwood and Jalufka[25] that there are appreciable drag forces on the plasma because of the momentum exchange between the ions and the cathode. The momentum transferred to a surface by a plasma component is determined by the product of the perpendicular particle current, the tangential momentum component, and the tangential momentum accommodation coefficient.

The existence of thresholds with respect to the B field and also with respect to the arc current suggests the onset of a new process. Initially at a given arc current, the velocity acquired by the plasma due to the magnetic field is small so that very little

momentum is transferred from the plasma to the electrode. Then at a certain critical value of B (or IxB) an appreciable momentum transfer from the plasma to the electrode begins to appear. This is demonstrated by the fact that a threshold in electrode drag is observed both as a function of B field and of arc current. Furthermore, the threshold B field is found to be approximately inversely proportional to the arc current in the range studied.

The existence of a threshold in the drag force indicates that there may be a threshold either in the tangential velocity, or in the particle current flow to the electrodes or in the momentum accommodation coefficient. These possibilities should be studied in more detail.

The detailed interpretation of the drag threshold has not yet been obtained. It is suggested, however, that the appearance of the threshold drag force is related to the sputtering threshold. The physical process of sputtering by high energy ions and atoms involves momentum transfer to the surface atoms. The sputtering yield and threshold are determined by the mass of the incident particle, the mass of the target particle, the properties of the target lattice, and the energy binding the target atoms to the surface. When the momentum transfer from the incoming particles is large enough to overcome the bond energies of the target atoms then there will be significant sputtering. At the same time it is expected that there will be a comperable threshold for momentum transfer to the target atoms. When the incident atom momentum transfer to a target atom is large enough to overcome lattice binding forces, the target atom can become mobile enough so that different lattice attractive forces are operative and so that the momentum accommodation coefficient changes . Since the energy required to make a target atom mobile on the surface will be less than the energy required to remove the target atom from the surface, the threshold for the accommodation coefficient change will be less than the threshold for sputtering. The similarity of the two processes suggests, however, that the accommodation coefficient threshold should be proportional to the sputtering threshold.

The results of the drag measurement can be interpreted in terms of a drag threshold energy proportional to the sputtering threshold energy. This is illustrated by comparing the drag force and sputtering thresholds for various combinations of gaseous ions and target materials.

Based upon conservation of momentum considerations the square of the plasma velocity (and therefore the kinetic energy) should be approximately proportional to the JxB force. The measured threshold force driving the plasma (proportional to JxB) and the published sputtering threshold[26] are listed in Table 1, which shows that the threshold ratios of argon on molybdenum relative to argon on copper for drag and for sputtering are 1.5 and 1.4 respectively. Also for a copper electrode the thresholds for measured drag as well as published sputtering appear to be independent of the mass of the ions. These observations indicate the similarity in the mechanism of the drag and the sputtering threshold.

Table 1

Drag Force and Sputtering Thresholds

Gas	Target	Drag Threshold (Amp x Kilogauss)	Sputtering[a] Threshold (ev)
Argon	Copper	16.5	17
Argon	Molybdenum	25.0	24
Helium	Copper	17.5	17[b]

(a) Stuart R. V. and Wehner, G. K., J. App. Phy., 33, 2345 (1962).

(b) Extrapolated from data in (a).

The use of improved accommodation coefficients together with better values of tangential ion velocity and the ion-cathode drag measurements can help one to deduce the ion current fraction at the cathode with better accuracy. The results can then be compared with a more detailed calculation of the electron emission based upon the ion-microfield emission model proposed for cold cathodes[1,2,9].

3.3 Determination of Tangential Velocity

As part of the interpretation of the data on tangential drag on electrodes by an accelerated plasma, it was necessary to study various aspects of the plasma phase and particle velocity. It was concluded that there is sometimes a large difference between the observed velocity of the plasma phase and the actual velocity of the plasma particles. The drag on the electrode is due to the momentum transfer by the ions and atoms themselves: But, unfortunately, the particle velocity is not as easily measured as that of the plasma phase velocity. It was shown in Section 2.3, for example, that for the low pressure range, where arc retrograde motion is frequently observed, the direction of plasma phase motion is opposite to that of the actual particle motion. Thus a measurement of the plasma phase velocity cannot really be used to determine the plasma particle velocity. An explanation of the retrograde motion is presented and shows that the plasma phase velocity is related to the growth and decay of plasma density.

In the absence of a direct measurement of ion velocity, the analysis of the electrode drag data was performed using the ionization limited velocity as indicated by Lin[27]. A preliminary study of the ionization limited velocity showed that the velocity is limited by the input power supplied to the arc and by the requirements of conservation of energy and of momentum: In this present program the concept of ionization limited velocity has been extended by the inclusion of the degree of ionization of the plasma as part of the model. Because of the anticipated need for the direct experimental determination of the particle velocity, a certain amount of time in this program has been devoted to an evaluation of

methods and difficulties involved in the direct measurement of ion and atom tangential velocity. Some of the results and recommendations are summarized in this section.

The back emf characteristic as a function of magnetic field has been used by some researchers[28,29] to estimate the plasma velocity. The velocity obtained from the V-B data has been interpreted by Lin[27] as the ionization limited velocity of the plasma. If this were the case, one should find V-B curve to be independent of gas pressure, the degree of ionization and other arc parameters for a given plasma gas. Our preliminary data, on the other hand, indicates that the slope (dV/dB), which is presumably proportional to the ionization limited particle velocity, varies considerably with gas pressure.

It was decided to study the Doppler shift method of measuring the velocity of a radiating particle, and to study some of the potential difficulties. The theory of Doppler effect states that the shift $\Delta\lambda$ in the wavelength λ from a source moving with a velocity v is given by,

$$\Delta\lambda = \lambda \frac{v}{c} \qquad (4)$$

where c is the velocity of light ($= 3 \times 10^{10}$ cm/sec). Thus if λ and $\Delta\lambda$ are measured from the experiment, one can estimate the velocity of the source. In a typical discharge, with a velocity v of the order of 10^6 cm/sec the expected shift $\Delta\lambda$ for a wavelength in the visible region ($\lambda \simeq 5,000$ Å) is of the order of 0.2 Å.

By selecting a particular characteristic wavelength λ from a given species in the arc plasma, it is possible to study the speed of that species in the plasma. This method can, therefore, measure the individual velocities of neutral gas, ion and other excited and radiating atoms in the arc. Because the radiation from the plasma is observed from a distance, the question of disturbing the flow pattern does not arise in this measurement as would be the case with probes or other sensors.

The instrumentation for the Doppler shift experiment is designed to suit the coaxial plasma accelerator that was used for the electrode drag force determination[2]. In this way the results of velocity measurement can be directly applied to interpret the results of drag measurement. An illustration of the apparatus for measuring λ and $\Delta\lambda$ from the arc is shown in Figure 4. Three light pipes are used to collect the radiation from the moving plasma. The central pipe looks at the radiation normal to the arc motion and does not record any Doppler shift. This acts as a reference signal. The other two pipes are inclined at 45° to observe a significant component of the velocity vectors along the line of sight. The radiation from a source moving towards or away from the observation point is collected by these pipes. A beam selector is located external to the vacuum system so that the signal from any one light pipe can be studied. Figure 4 shows the construction of the molybdenum electrode with high temperature alumina insulation. The fiber optics is mounted on the electrode shaft itself to bring the light signal out of the vacuum chamber. The other electrode consists of a water-cooled copper ring placed symmetrically around the central electrode.

The light from the plasma is thus collected with fiber optics located in the vicinity of the central electrode. They are placed close to the plasma so that a small volume of plasma is sampled,thus resulting in a better defined signal with minimum scatter. Due to the excessive heat in the proximity of the plasma, the commercial light pipes (epoxy sealed) could not be used without a complicated cooling system. This difficulty was overcome by using solid light pipes of borosilicate glass. The transmission efficiency of these fibers was estimated to be about 90% per foot in the range of 0.3 to 3 microns.

The light pipes of glass rod of 1/8 inch diameter with polished ends and desired shapes were mounted in the plasma generator using vacuum O-ring seals which were found satisfactory for this application. With this system, the arc was operated continuously for periods over 15 minutes without any noticeable damage to the electrodes and the optical system. Outside the

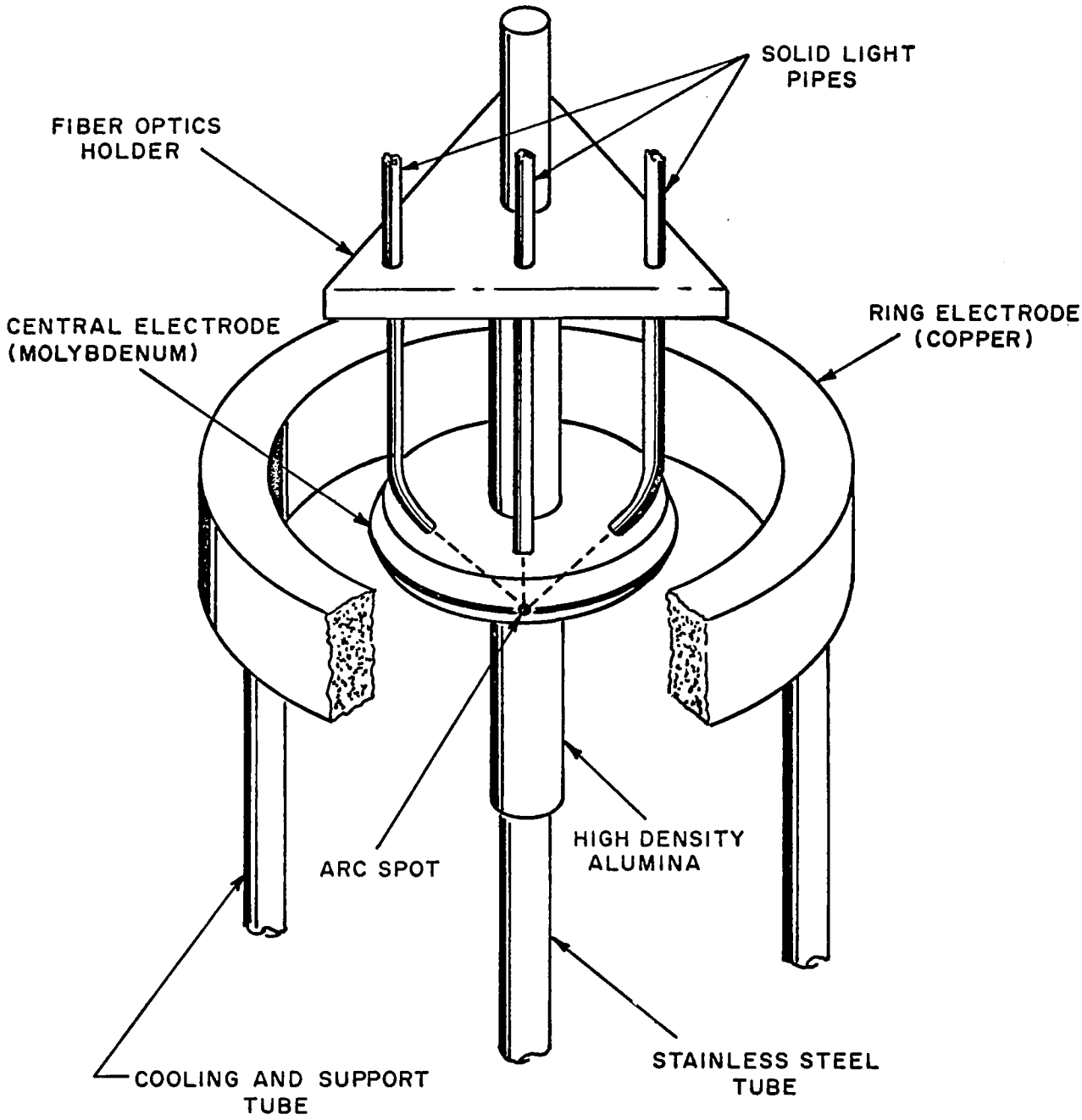

FIGURE 4.

ELECTRODE GEOMETRY AND FIBER OPTIC ARRANGEMENT FOR THE MEASUREMENT OF PARTICLE VELOCITY BY THE DOPPLER SHIFT METHOD.

vacuum chamber, Bausch and Lomb fiber optics of 1/4 inch diameter were used to transport the light to an optical discriminator. A number of designs for the optical discrimination have been considered. Basically the device should give an output voltage which is dependent upon the wavelength change and is independent of changes of amplitude. The various discriminator designs will not be described here. The sensitivity of the system can be improved by using cooled photodetectors to reduce noise and dark current. Further noise reduction can be obtained by chopping the optical signal, with the subsequent recovery of the information using a phase sensitive detector.

It is recommended that further effort be devoted to developing a Doppler shift instrument for the measurement of plasma particle velocity in the plasma configuration used for the electrode drag measurements.

4. SUMMARY

The theoretical work described in Section 2.1 has extended the new sheath model by including a transverse plasma flow outside the sheath region and has thus established a self-consistent approach for the plasma sheath problem in the collisionless limit.

One major contribution of the new sheath model lies in the incorporation of very general microscopic boundary conditions at the electrode as well as in the better representation of the particle distribution functions at the sheath edge. Consequently, any possible plasma-boundary interactions can be taken into account in the new sheath model; the usual limitations of other sheath models such as the assumptions of monoenergetic particles and total annihilation of particles at the electrode are now entirely removed.

The new sheath model also reveals the importance of the accommodation coefficients at the boundary surface.

The investigation reported in Section 2.2 represents a first attempt in the direction to understand the effects of collisions and ionizations in the plasma sheath from a kinetic theory approach. Because of the complexity of the problem as well as the numerous parameters involved, only a brief discussion of the motivation is given in Section 2.2. Detailed analysis is carried out in Ref. 4 . The result obtained in the present study for the effects of the ionization process indicates the possibly large variation of the current partition in the sheath. Other results such as the importance of the electron generation and the dependence of the sheath structure on the degree of ionization are also discussed in Ref. 4. Obviously, all these collision and ionization effects will be more pronounced as the sheath thickness becomes comparable to the mean free paths.

The measured drag at the cathode and anode electrodes, for the case of a magnetically accelerated plasma, has been interpreted to deduce more information

about the physical processes occurring at the plasma-electrode interface. Of particular concern is the implication of the observed threshold for tangential force as a function of transverse magnetic field and of arc current. The results suggest the possibility of a threshold in the tangential momentum accommodation coefficient. The existance of a threshold accommodation coefficient can be explained in terms of an atom displacement threshold, which should be proportional to the sputtering threshold for removal of atoms from the surface.

The theory of plasma and particle propagation was analyzed in conjunction with the problem of retrograde arc motion. A model was proposed to explain retrograde motion as retrograde plasma phase motion, rather than as retrograde particle motion. It appears that the retrograde motion in a transverse magnetic field can be explained as the enhanced growth of plasma density in the region of larger total magnetic field: This is due to the inhibited diffusion loss of ions and electrons as a result of a larger magnetic field. It was therefore shown, that the plasma phase velocity does not necessarily correspond to the velocity of the plasma particles.

Because of the need for the measurement of tangential particle velocities (in order to aid the further interpretation of the electrode drag measurements), a Doppler shift method for the direct measurement of ion and atom velocity was devised. Some design considerations and suggestions are briefly described. More accurate data for the tangential particle velocity together with better values for the accommodation coefficient can aid in the interpretation of the drag measurements. An example is the improved evaluation of the ion current partitioning at the cathode spot. This result can then be compared with the predictions of the ion micro-field emission model proposed to explain electron emission in cases where thermionic or field emission are not applicable at cold cathodes.

ACKNOWLEDGMENT

This research was supported by the National Aeronautics and Space Administration under Contract NASw-1014 to Space Sciences Incorporated (1966 to 1967). It is our pleasure to express our gratitude to the National Aeronautics and Space Administration for their financial support, and to Professor H. Grad of the Courant Institute of New York University for his many valuable suggestions and constructive comments throughout the program. In addition, we are happy to acknowledge the suggestions of Dr. K. Thom and his co-workers of the National Aeronautics and Space Administration leading to the basic concept for the electrode drag measurement experiment. The skillful assistance of Mr. James Dodge, Mr. George Leonard and of Miss Ellen Parent has been of considerable value.

REFERENCES

1. Aisenberg, S., Hu, P.N., Rohatgi, V. K. and Ziering, S., "A Study of Electrode Effects in Crossed Field Accelerators," Summary Report, Space Sciences Document SSI-152-SR (September 1965).

2. Aisenberg, S., Hu, P.N., Rohatgi, V. K. and Ziering, S., "Plasma Boundary Interactions," NASA Contractor Report, NASA CR-868, Washington, D. C. (August 1967).

3. Hu, P. N. and Ziering, S., "Collisionless Theory of a Plasma Sheath Near an Electrode," Phys. Fluids, 9, 2168 (1966).

4. Hu, P. N. and Ziering, S., "Collisionless Plasma Sheath with Transverse Flow," Tech. Rept. 406-4, Space Sciences Incorporated (1967). Accepted for publication in the Physics of Fluids in a condensed form.

5. Hu, P. N. and Ziering, S., "Kinetic Model of Three-Component Plasmas with Ionization," Phys. Fluids, 9, 1983 (1966).

6. Hu, P. N. and Ziering, S., "Collision and Ionization Effects in a Plasma Sheath," Tech. Rept. 406-13, Space Sciences Incorporated (1967). Accepted for publication in the Journal of Plasma Physics.

7. Hu, P. N. and Ziering, S., "Collisionless Plasma Sheath with Transverse Flow." Presented at the Eighth Annual Meeting of the Plasma Physics Division, American Physical Society, Boston, Mass. (November 1966).

8. Rohatgi, V. K. and Aisenberg, S., "Tangential Momentum Transfer to the Electrodes of a Magnetically Accelerated Arc." Presented at the Eighth Annual Meeting of the Plasma Physics Division, American Physical Society, Boston, Mass. (November 1966).

9. Aisenberg, S. and Rohatgi, V. K., "A Study of Electron Emission Processes at Arc Cathodes." Presented at the Eighth Annual Meeting of the Plasma Physics Division, American Physical Society, Boston, Mass. (November 1966).

10. Aisenberg, S., "Plasma Propagation Theory of Arc Retrograde Motion." Presented at the Eighth Symposium on the Engineering Aspects of MHD (March 1967).

11. Rohatgi, V. K. and Aisenberg, S., "Ion Drag and Current Partitioning at the Cathode of a Plasma Accelerator," AIAA Paper No. 67-657. AIAA Electric Propulsion and Plasma Dynamics Conference, Colorado (September 1967).

12. Stark, J., Physik. Z. 4, 440 (1903).

13. Sommerville, J. M., The Electric Arc (Methuen and Co., Ltd., London, 1959) p. 82.

14. Afshartous, S. B., Aisenberg, S., Rohatgi, V. and Smith, C. G., "Investigation of Cathode Phenomena in the Mercury Arc," Technical Report RADC-TR-66-12 (February 1966).

15. Allis, W. P., "Motion of Ions and Electrons," Handbuch der Physik, Vol. 21 (Springer, Berlin, 1956).

16. Kesaev, I. G., Cathode Processes in the Mercury Arc (Consultants Bureau, N.Y., 1964) p. 251.

17. Ecker, G., and Müller, K. G., J. Appl. Phys. 29, 1606 (1958).

18. Hernquist, K. G., and Johnson, E. O., Phys. Rev. 98, 1576 (1955)

19. Guile, A. E., Lewis, T. J., and Mehta, S. F., Brit. J. Appl. Phys. 8, 444 (1957).

20. St. John, R. M. and Winans, I. G., Phys. Rev. 94, 1097 (1954).

21. Gallagher, C. J., J. Appl. Phys. 21, 768 (1950).

22. Smith, C. G., Phys. Rev. 63, 217 (A) (1943).

23. Roman, W. C., 6th International Conference on Ionization Phenomena in Gases, Paris, 1963.

24. Aisenberg, S. and Rohatgi, V. K., Appl. Phys. Letters, 8, 194 (1966).

25. Thom, K., Norwood, J., and Jalufka, N., Phys. Fluids, S67 (1964).

26. Stuart, R. V. and Wehner, G. K., J. Appl. Phys., 33, 2345 (1962).

27. Lin, S. C., Phys. Fluids, 4, 1277 (1961).

28. Fahleson, V., Phys. Fluids, 4, 123 (1966).

29. Patrick, R. and Schneiderman, A., Sixth Symposium on Engineering Aspect of MHD, Pittsburgh (1965).

APPENDIX A

COLLISIONLESS PLASMA SHEATH WITH TRANSVERSE FLOW

(By: Pung Nien Hu and Sigi Ziering)

ABSTRACT

The problem of the transverse plasma sheath is examined by imposing microscopic boundary conditions for the surface-particle interactions. Explicit expressions for the physical quantities of interest are derived in the general case, and detailed calculations are made for a special case for which a simple analytic solution for the sheath structure is obtained. The most important result is, that the retarding effect of the electrode on the transverse velocity of the accelerated particles may extend well beyond the distance of the sheath thickness (defined in the usual sense) for high potential drops across the sheath. Specific analytic expressions for the ion and electron drag at the cathode are obtained. The theory developed can be used to calculate various slip coefficients.

1. INTRODUCTION

Historically the problem of the plasma sheath was formulated in connection with gaseous discharge phenomena. For those applications any existing mass flow of the various particle species would be in a direction normal to the surface (electrode). More recently, a large amount of analytical effort in support of diagnostic measurements by electric probes has considered sheath theory, but again under normal flow conditions. The advent of space flight however has brought to the foreground many practical applications for the ionized counterparts of the well known problems of Couette Flow, Poiseulle Flow and Kramer's Problem in the kinetic theory of gases. All of these problems have a common feature, that is the flow of a plasma past a surface. Specifically, plasma machines (both generators and accelerators) and space flight itself through an ionized medium (as for instance the Solar Wind) are practical applications in which the interactions with the surface of a plasma flowing parallel to the surface are of critical importance. It is these latter problems which motivate the present investigation of the transverse plasma sheath. The former problems characterized by a normal net flow to the surface have been considered in a previous paper[1] (hereafter referred to as I).

As in neutral gases there is always a collisionless domain near a physical boundary, irrespective of whether the bulk flow is normal or parallel to the surface. The physical surface introduces discontinuities in the particle distribution function, which will eventually be wiped out through the randomizing effect of collisions, but not in the sheath itself. These discontinuities are a result of the classical effects leading to slip considerations, that is the characteristic temperatures and flow velocities of the surface differ from those of the plasma. In addition, consideration

of charged particles accentuates these discontinuities due to the preferential effect of the local electromagnetic force field on the different species, as well as charge transfer and particle emission and absorption at the boundary. The sum of all these effects would indicate that the particle distribution functions near a physical boundary are much more singular for ionized gases than they are for neutral gases. It is therefore not surprising that experimentally significant gradients of the electric field in the sheath are observed.

In order to incorporate these discontinuities into the theory, special techniques have been developed more recently for application to kinetic theory[2]. The techniques of separating the distribution functions in accordance with particles approaching and receding from the surface have been successful to yield theoretical slip coefficients[3,4], and have been generally found useful in a variety of kinetic theory problems in which the incorporation of microscopic boundary conditions was of importance. It is our intent to apply similar techniques to the sheath problem, which in view of the above discussion should be much more sensitive to the incorporation of microscopic boundary conditions. At the same time these techniques are also more relevant for a better physical understanding and application of theory to practical problems. Thus the present solution allows the calculation of momentum transfer to the electrode, and this can be directly applied to some recent experimental measurements by Aisenberg and Rohatgi[5] of electrode drag.

Ideally one would like to develop a theory equally valid and applicable to the sheath as well as the bulk of the plasma, that is extending from collisionless to continuum flows. The success achieved in neutral gas dynamics for a class of geometrically simple and linearized problems of obtaining analytic solutions spanning the whole domain would hold forth promise. The complexity of multiple coupled kinetic equations and the

simultaneous requirement of satisfying Maxwell's equations, however, hold little hope of obtaining uniformly valid solutions. It is therefore our objective to treat rigorously the transverse sheath assuming a variety of microscopic boundary conditions. Subsequent to this analysis the sheath solution will yield boundary conditions for the continuum solution. This will at least assure that the rapid changes of the distribution function in the sheath have been adequately represented. At the same time, once the sheath domain has been covered adequately, the continuum representation for the remaining domain should be excellent. Thus we are proposing a piecewise analytic approach, the first part herein considered consists of the sheath structure in which the microscopic boundary conditions at the surface are incorporated in a rigorous and self-consistent way. This will allow us to account for the major singularities in the distribution function, and arrive at proper boundary conditions for the continuum domain after the rapidly changing and non-continuum behaviour has been separated. Thus a proper sheath theory will allow us to approach the continuum domain with a set of physically realistic boundary conditions.

The problem considered is that of an infinite planar surface, and a plasma flowing past this surface under steady-state conditions. The surface can be either an insulator or a conductor, and we will assume sufficient parameters to be able to impose microscopic boundary conditions on the respective species, that is we specify whether the charged and neutral particles are reflected, emitted, absorbed, or neutralized at the surface. This is an all-inclusive set of boundary conditions and not limited by the customary assumption that charged particles are either completely absorbed or neutralized at the surface. We assume that at the sheath-plasma boundary a continuum flow exists, that is we assume that the flow velocities, temperatures and densities of the various species can be specified. It is then part of our task for the sheath problem to relate these latter parameters to the boundary conditions imposed at the surface. We do not imply however, that

the flow variables past the sheath remain constant, what we do specify is that the plasma starting at the sheath boundary can be specified by a near-equilibrium distribution function such as a displaced Maxwellian or a Chapman-Enskog expansion. Thus the crucial problem as we see it is to relate the parameters or boundary conditions at the plasma-sheath interface to those at the sheath-surface.

The assumed electron and ion distribution functions for a cathode will be given in the next section. Section 2 will consider the cathode for the purpose of illustrating the method, the extension to the anode is straightforward. The general expressions for plasma properties in the sheath will be derived in Section 3. The special cases where the component temperatures of the electrons, the ions and the electrode are identical and for which a simple analytic solution was obtained in I will be treated in Section 4. The results will then be discussed in Section 5.

Notation used in I will be followed in the present paper unless otherwise specified.

2. DISTRIBUTION FUNCTIONS

As stated in the introduction, we are assuming a plasma moving past an infinite planar surface in order to examine the sheath properties between the fully developed continuum flow and the bounding surface. We assume that the mean free paths as well as the Larmor radii of the electrons and ions are large compared with the Debye length. The electric potential satisfies Poisson's equations (I:1) and the distribution functions for the electrons and ions in the sheath satisfy the respective Vlasov equations (I:2). We further assume that the transverse velocity component of the plasma can be taken into account by expressing the distribution functions as displaced Maxwellians. Thus, for a cathode, particles can be divided into various groups depending on their trajectories (I: Figs. 1 and 2) and their distribution functions, identified by their total energies, can be expressed as:

$$f_1^- = \left(\frac{a^-}{\pi}\right)^{3/2} c^- H(\epsilon - e^-\phi)\, H(e^-\phi_o - \epsilon) \exp\left\{-\frac{\epsilon - e^-\phi_1}{kT^-} - a^-\left[(\eta - \tilde{V}^-)^2 + \zeta^2\right]\right\} \tag{1}$$

$$f_2^\pm = \left(\frac{a^\pm}{\pi}\right)^{3/2} c^\pm H(\epsilon - e^\pm\phi)\, H(\epsilon - e^\pm\phi_o)\, H(-\xi) \exp\left\{-\frac{\epsilon - e^\pm\phi_1}{kT^\pm} - a^\pm\left[(\eta - \tilde{V}^\pm)^2 + \zeta^2\right]\right\} \tag{2}$$

$$f_3^\pm = \alpha_1^\pm \left(\frac{a^\pm}{\pi}\right)^{3/2} c^\pm H(\epsilon - e^\pm\phi)\, H(\epsilon - e^\pm\phi_o)\, H(\xi) \exp\left\{-\frac{\epsilon - e^\pm\phi_1}{kT^\pm} - a^\pm\left[(\eta - \tilde{V}^\pm)^2 + \zeta^2\right]\right\} \tag{3}$$

$$f_4^+ = \left(\frac{a_o^+}{\pi}\right)^{3/2} c_o^{\pm}\, H(\epsilon - e^+\phi)\, H(e^+\phi_1 - \epsilon) \exp\left\{-\frac{\epsilon - e^+\phi_0}{kT_o} - a_o^+(\eta^2+\zeta^2)\right\} \qquad (4)$$

$$f_5^{\pm} = \left(\frac{a_o^{\pm}}{\pi}\right)^{3/2} c_1^{\pm}\, H(\epsilon - e^{\pm}\phi)\, H(\epsilon - e^{\pm}\phi_1)\, H(\xi) \exp\left\{-\frac{\epsilon - e^{\pm}\phi_0}{kT_o} - a_o^{\pm}(\eta^2+\zeta^2)\right\} \qquad (5)$$

$$f_6^- = \gamma^- \left(\frac{a_o^-}{\pi}\right)^{3/2} c^-\, H(\epsilon - e^-\phi)\, H(\epsilon - e^-\phi_1)\, H(\xi) \exp\left\{-\frac{\epsilon - e^-\phi_0}{kT_o} - a_o^-(\eta^2+\zeta^2)\right\} \qquad (6)$$

where,

$$a^{\pm} = m^{\pm}/2kT^{\pm}$$

$$a_o^{\pm} = m^{\pm}/2kT_o$$

$$\epsilon = \frac{1}{2} m^{\pm} \xi^2 + e^{\pm} \phi(x) .$$

In the above expressions, ϕ_0 and ϕ_1 are the potentials at the electrode and the sheath edge, respectively, distribution functions f_1^-, $f_2^{\pm}$, and $f_3^{\pm}$ which represent particles coming from the sheath edge have constant transverse velocity components $\tilde{V}^{\pm}$ in the y-direction, while distribution functions f_4^+, $f_5^{\pm}$, and f_6^- represent particles coming from the cathode which do not have a transverse velocity component.

In the present case, T^+ and T^-, defined as the component temperatures of the ions and the electrons, respectively, reduce to the usual temperatures as either the transverse velocities vanish or all particles are specularly reflected from the electrode.

Obviously, the above distribution functions satisfy the respective Vlasov equations (I:2). Furthermore, since the inclusion of the transverse velocity components $\tilde{V}^{\pm}$ does not alter the number densities of the electrons and ions at any point, the constants $c_0^{\pm}$, $c_1^{\pm}$, and $c^{\pm}$ are identical with those determined in Section 3 of I and the possible ranges of the emission and reflection coefficients of the cathode for the existence of a monotonic sheath structure are the same as determined in Section 5 of I. It then remains to determine the velocity profile of $\tilde{V}^{\pm}$ in the sheath from the actual transverse velocity components of the electrons and ions at the sheath edge.

To integrate the distribution functions, we note that the range of integration is given by;

$$e^{\pm}\phi_0 \leq \epsilon \leq \infty$$

for particles coming from the electrode, and

$$e^{\pm}\phi_1 \leq \epsilon \leq \infty$$

for particles coming from the sheath edge. Multiplying the distribution functions by η and integrating over the velocity space in the appropriate ranges, we have the momentum flow for the ions in the y-direction

$$n^+ v^+ = (n_2^+ + n_3^+)\tilde{V}^+ \tag{7}$$

where n_2^+ and n_3^+, respectively represent the number densities of the distribution functions f_2^+ and f_3^+, which are obtained in I as;

$$n_2^+ = \frac{1}{2} c^+ \exp\left[\frac{e^+(\phi_1-\phi)}{kT^+}\right] \text{erf c}\left[\frac{e^+(\phi_1-\phi)}{kT^+}\right]^{1/2}$$

and $n_3^+ = \alpha_1^+ n_2^+$.

At the sheath edge, $\phi = \phi_1$ and we have

$$n^+ v^+ = N^+ V^+ = \frac{1}{2} (1 + \alpha_1^+) c^+ \tilde{V}^+ \tag{8}$$

which determines the transverse velocity component $\tilde{V}^+$ in the distribution functions f_2^+ and f_3^+ from the actual transverse velocity component V^+ of the ions at the sheath edge.

The transverse ion momentum can now be written as;

$$n^+ v^+ = N^+ V^+ \exp\left[\frac{e^+(\phi_1 - \phi)}{kT^+}\right] \text{erf c}\left[\frac{e^+(\phi_1 - \phi)}{kT^+}\right]^{1/2} \tag{9}$$

which only depends on the cathode parameters implicitly through the potential.

Similarly, we have the momentum of the electrons in the y-direction.

$$n^- v^- = (n_1^- + n_2^- + n_3^-) \tilde{V}^- \tag{10}$$

where,

$$n_1^- = c^- \exp\left[\frac{e^-(\phi_1 - \phi)}{kT^-}\right] \operatorname{erf}\left[\frac{e^-(\phi_0 - \phi)}{kT^-}\right]^{1/2}$$

$$n_2^- = \frac{1}{2} c^- \exp\left[\frac{e^-(\phi_1 - \phi)}{kT^-}\right] \operatorname{erf} c\left[\frac{e^-(\phi_0 - \phi)}{kT^-}\right]^{1/2}$$

and

$$n_3^- = \alpha^- n_2^-.$$

At the sheath edge, we have,

$$n^- v^- = N^- V^- = c^- \tilde{V}^- \left\{1 + \frac{1}{2}(\alpha^- - 1) \operatorname{erf} c\left[\frac{e^-(\phi_0 - \phi_1)}{kT^-}\right]^{1/2}\right\} \qquad (11)$$

which determines the transverse velocity component $\tilde{V}^-$ in the distribution functions f_1^-, f_2^-, and f_3^- from the actual transverse component V^- of the electrons at the sheath edge.

With the transverse velocity components $\tilde{V}^{\pm}$ given by Eqs. (8) and (11) and the other plasma parameters as well as the possible ranges of the emission and reflection coefficients of the electrode determined in I, we now have the distribution functions as expressed in Eqs. (1) through (6) completely determined in terms of the potential $\phi(x)$ which can be found by a numerical integration of the electric field given by (I:43). Other plasma properties can then be calculated from the integration of the distribution

functions over the velocity space. Evidently, any plasma property that does not involve the velocity moment of the distribution functions in the y-direction will be the same as that evaluated in I. In the next section, we will carry out those plasma properties that have been altered because of the inclusion of the transverse velocity components of the electrons and ions.

3. GENERAL EXPRESSIONS

In general, ions are not completely reflected from the cathode, some of them are therefore neutralized by the electrode and are then emitted as neutral particles. In the plasma outside the sheath, there are always neutral particles because the ionization process is seldom complete. The presence of neutral particles near the electrode as well as outside the sheath, although it does not have any effect on the electric field and current and therefore will not change the basic structure of the sheath, does make the evaluation of some of the plasma properties more difficult. Specifically, many plasma properties, such as the pressure, the temperature, and the heat flow, depend on the distribution function of the individual components of the plasma as well as the mass velocity of the entire plasma. From the momentum conservation law, we can readily conclude that the velocity component of the plasma normal to the electrode must be zero (or negligibly small) if we assume that no particles (or only electrons) are annihilated at the electrode. Without a transverse velocity component of the plasma, we are therefore able to evaluate the partial pressures and heat flows of the electrons and ions as in I. In the present paper, we will derive the expressions for the individual quantities as well as the partial physical quantities for the electrons and the ions and we will evaluate those terms that depend on the sheath structure.

The individual electron and ion pressures are defined as:

$$3\,\bar{p}^{\pm} = m^{\pm} \int \left[(\xi - u^{\pm})^2 + (\eta - v^{\pm})^2 + \zeta^2 \right] f^{\pm}\, d\underset{\sim}{\xi}$$

where the integration over the velocity space is to be carried out in the full range of η and ζ but in different ranges of ξ as specified in the preceding section.

Denoting

$$f^{\pm}_{xx} = \int \xi^2 f^{\pm} d\underset{\sim}{\xi}\,, \quad f^{\pm}_{yy} = \int \eta^2 f^{\pm} d\underset{\sim}{\xi}\,, \quad \text{etc.}$$

we then have,

$$3\bar{p}^{\pm} = m^{\pm}\left(f^{\pm}_{xx} + f^{\pm}_{yy} + f^{\pm}_{zz}\right) - m^{\pm} n^{\pm} (u^{\pm})^2 - m^{\pm} n^{\pm} (v^{\pm})^2 \qquad (12)$$

the partial pressures of electrons and ions are defined as,

$$3p^{\pm} = m^{\pm} \int \left[\xi^2 + (\eta - v)^2 + \zeta^2\right] f^{\pm} d\underset{\sim}{\xi}$$

where v is the velocity component in the y-direction of the plasma when considered as a fluid and where we have used the fact that the velocity component of the plasma in the x-direction is identically zero.

Again we may express

$$3p^{\pm} = m^{\pm}\left(f^{\pm}_{xx} + f^{\pm}_{yy} + f^{\pm}_{zz}\right) + m^{\pm} n^{\pm} v (v - 2v^{\pm}), \qquad (13)$$

so that the total pressure of the plasma can be obtained by summing up the partial pressures of the electrons, the ions and the neutral particles.

Similarly, the individual heat flows in the x- and y-directions can be expressed respectively as,

$$2\bar{Q}_2^{\pm} = m^{\pm} \int \left[(\xi - u^{\pm})^2 + (\eta - v^{\pm})^2 + \zeta^2 \right] (\xi - u^{\pm})\, f^{\pm}\, d\underset{\sim}{\xi}$$

$$= m^{\pm} \left(f^{\pm}_{xxx} + f^{\pm}_{xyy} + f^{\pm}_{xzz} \right) - 3\bar{p}^{\pm} u^{\pm} - 2m^{\pm} \left(u^{\pm} f^{\pm}_{xx} + v^{\pm} f^{\pm}_{xy} \right)$$

$$+ m^{\pm} n^{\pm} u^{\pm} \left[(u^{\pm})^2 + (v^{\pm})^2 \right] \qquad (14)$$

and

$$2\bar{Q}_y^{\pm} = m^{\pm} \int \left[(\xi - u^{\pm})^2 + (\eta - v^{\pm})^2 + \zeta^2 \right] (\eta - v^{\pm})\, f^{\pm}\, d\underset{\sim}{\xi}$$

$$= m^{\pm} \left(f^{\pm}_{xxy} + f^{\pm}_{yyy} + f^{\pm}_{yzz} \right) - 3\bar{p}^{\pm} v^{\pm} - 2m^{\pm} \left(u^{\pm} f^{\pm}_{xy} + v^{\pm} f^{\pm}_{yy} \right)$$

$$+ m^{\pm} n^{\pm} v^{\pm} \left[(u^{\pm})^2 + (v^{\pm})^2 \right] \qquad (15)$$

The respective partial heat flows can be expressed as

$$2Q_x^{\pm} = m^{\pm} \int \left[\xi^2 + (\eta - v)^2 + \zeta^2 \right] \xi\, f^{\pm}\, d\underset{\sim}{\xi}$$

$$= m^{\pm} \left(f^{\pm}_{xxx} + f^{\pm}_{xyy} + f^{\pm}_{xzz} \right) - 2m^{\pm} v\, f^{\pm}_{xy} + m^{\pm} n^{\pm} u^{\pm} v^2 \qquad (16)$$

and

$$2Q_y^{\pm} = m^{\pm} \left(f^{\pm}_{xxy} + f^{\pm}_{yyy} + f^{\pm}_{yzz} \right) - 3p^{\pm} v - 2m^{\pm} v\, f^{\pm}_{yy} + m^{\pm} n^{\pm} v^{\pm} v^2 \qquad (17)$$

Finally, the drag forces on the electrode per unit area due to the ions and electrons can be expressed as

$$D^{\pm} = - m^{\pm} \int \xi\eta\, f^{\pm}\, d\underset{\sim}{\xi} = - m^{\pm}\, f^{\pm}_{xy} \tag{18}$$

In the above expressions (Eqs. (12) through (18)), $n^{\pm}$ and $u^{\pm}$ have been evaluated in I, while $v^{\pm}$ have been evaluated in the preceding section. Other moments can be easily evaluated from the respective distribution functions given in the preceding section. The results are:

$$m^{+} f^{+}_{xx} = m^{+} f^{+}_{zz} + \left[c^{+}\sqrt{T}^{+}\left(1+\alpha^{+}_{1}\right)+\left(c^{+}_{1}-2c^{+}_{0}\right)\sqrt{T}_{0}\exp\left(-aT^{-}/T_{0}\right)\right]\left[k\,e(\phi_{1}-\phi)/\pi\right]^{1/2}$$

$$m^{-} f^{-}_{xx} = m^{-} f^{-}_{zz} + c^{-}\left[\sqrt{T}^{-}\, e^{-a}(\alpha^{-}-1)+\sqrt{T}_{0}\,(\beta^{-} e^{-a}+\gamma^{-})\right]\left[k\,e\,(\phi-\phi_{0})/\pi\right]^{1/2}$$

$$m^{\pm} f^{\pm}_{yy} = m^{\pm} f^{\pm}_{zz} + m^{\pm}\,(\tilde{V}^{\pm})^{2}\left(n^{\pm}_{1} + n^{\pm}_{2} + n^{\pm}_{3}\right)$$

$$m^{\pm} f^{\pm}_{zz} = kT^{\pm}\left(n^{\pm}_{1} + n^{\pm}_{2} + n^{\pm}_{3}\right) + kT_{0}\left(n^{\pm}_{4} + n^{\pm}_{5} + n^{\pm}_{6}\right)$$

$$m^{+} f^{+}_{xy} = c^{+}\tilde{V}^{+}\left(\alpha^{+}_{1} - 1\right)\left(m^{+}\, kT^{+}/2\pi\right)^{1/2}$$

$$m^{-} f^{-}_{xy} = c^{-}\tilde{V}^{-}\, e^{-a}\left(\alpha^{-} - 1\right)\left(m^{-}\, kT^{-}/2\pi\right)^{1/2}$$

$$m^{\pm}\left(f^{+}_{xxx}+f^{+}_{xyy}+f^{+}_{xzz}\right)=c^{+}\left(\alpha^{+}_{1}-1\right)\left(\frac{2kT^{+}}{\pi m^{\pm}}\right)^{1/2}\left[e(\phi_1-\phi)+2kT^{+}+\frac{1}{2}\,m^{+}\,(\tilde{V}^{+})^2\right]$$

$$+c^{+}_{1}\left(\frac{2kT_0}{\pi m^{+}}\right)^{1/2}\left[e(\phi_1-\phi)+2kT_0\right]\exp\left(-aT^{-}/T_0\right)$$

$$m^{-}\left(f^{-}_{xxx}+f^{-}_{xyy}+f^{-}_{xzz}\right)=c^{-}\,e^{-a}\,(\alpha^{-}-1)\left(\frac{2kT^{-}}{\pi m^{-}}\right)^{1/2}\left[e(\phi-\phi_0)+2kT^{-}+\frac{1}{2}\,m^{-}(\tilde{V}^{-})^2\right]$$

$$+c^{-}\left(\beta^{-}\,e^{-a}+\gamma^{-}\right)\left(\frac{2kT_0}{\pi m^{-}}\right)^{1/2}\left[e(\phi-\phi_0)+2kT_0\right]$$

$$m^{+}\left(f^{+}_{xxy}+f^{+}_{yyy}+f^{+}_{yzz}\right)=\tilde{V}^{+}\left(n^{+}_{2}+n^{+}_{3}\right)\left[5kT^{+}+m^{+}\,(\tilde{V}^{+})^2\right]$$

$$+c^{+}\tilde{V}^{+}\left(1+\alpha^{+}_{1}\right)\left[ekT^{+}\,(\phi_1-\phi)/\pi\right]^{1/2}$$

$$m^{-}\left(f^{-}_{xxy}+f^{-}_{yyy}+f^{-}_{yzz}\right)=\tilde{V}^{-}\left(n^{-}_{1}+n^{-}_{2}+n^{-}_{3}\right)\left[5kT^{-}+m^{-}\,(\tilde{V}^{-})^2\right]$$

$$+c^{-}\tilde{V}^{-}\,e^{-a}\,(\alpha^{-}-1)\left[ekT^{-}\,(\phi-\phi_0)/\pi\right]^{1/2}$$

where,

$$a=e\,(\phi_1-\phi_0)/kT^{-}$$

$$n^{+}_{1}=n^{-}_{4}=n^{+}_{6}=0$$

$$n_5^- = \frac{1}{2}\beta^- c^- \exp\left[-\frac{e(\phi_1 - \phi)}{kT_0}\right] \operatorname{erf} c\left[\frac{e(\phi - \phi_0)}{kT_0}\right]^{1/2}$$

and

$$n_6^- = \frac{1}{2}\gamma^- c^- \exp\left[-\frac{e(\phi - \phi_0)}{kT_0}\right] \operatorname{erf} c\left[\frac{e(\phi - \phi_0)}{kT_0}\right]^{1/2}.$$

Other quantities are given in the preceding section and I. In the above results, we have expressed all quantities in dimensional forms.

From the above results, the individual pressures, heat flows and drag forces of the electrons and ions, as given in Eqs. (12) through (19) can be calculated by a straight forward substitution in terms of the potential which, in turn, can be calculated by a quadrature subject to the electrode and plasma parameters. However, we have shown in I that the potential is a monotonic function of the distance normal to the electrode and the electric field is strongest at the electrode, therefore much useful information can be deduced from the above results without knowing the exact potential profile.

It is interesting to observe that the drag force (or the skin friction) at the cathode due to the ions can now be expressed as,

$$D^+ = N^+ V^+ \left(\frac{1 - \alpha_1^+}{1 + \alpha_1^+}\right)\left(\frac{2m^+ kT^+}{\pi}\right)^{1/2}$$

which shows that the ion drag force does not depend explicitly on the potential difference across the sheath although the coefficient α_1^+ may implicitly do so. This therefore suggests that the threshold effect of

the drag force on a cathode as observed by Aisenberg and Rohatgi[5] is unlikely to be caused by any mechanism occuring inside the sheath; it may be caused by some phenomena outside the sheath.

On the other hand, the electron drag force can be expressed as,

$$D^- = \frac{N^- V^- e^{-a} (1 - \alpha^-)(2m^- kT^-/\pi)^{1/2}}{2 - (1 - \alpha^-) \text{ erf } c\sqrt{a}}$$

which decreases monotonically with an increasing potential difference across the sheath.

Another interesting result is that the shear stresses of the ion and electrons are constant throughout the sheath, however, the vorticities are not as can be seen from Eqs. (9) and (10). A further examination shows that the variation of vorticities is caused by the mechanism of diffuse ion and electron reflections and is therefore a unique result of the present sheath model.

Despite the fact that there are no collisions between particles inside the sheath, variations of the transverse velocity components and the temperature of the ions and electrons are found in the sheath because of the effect of the electric field as well as the diffuse reflections from the electrode. The velocity and temperature slips for ions and electrons can be calculated for the sheath in the same fashion as was done by Gross and Ziering[3] and Ziering[4] for neutral gases. As in Ref. I, we will treat a special case in the next section, which allows for some analytical insight.

4. A SPECIAL CASE

The expressions for the individual flow properties for the ions and electrons derived in the preceding section are quite general. Once the electrode and the plasma parameters are specified, all physical quantities can be readily calculated. However, in view of the great variety of parameters, it is difficult to make calculations for the general case. As an illustration, a special case for which a simply analytic solution has been obtained in I will be treated in this section to include the effect of the transverse velocity components.

The special case occurs when 1) the component temperatures for the ions, the electrons, and the electrode are the same; 2) there is neither a net charge nor an electric field at the sheath edge; 3) the trapped ions near the cathode only undergo specular reflections; and 4) the electrons are completely reflected from the cathode which, in addition, does not emit particles. In this case, the potential profile can be integrated explicitly. Quantities that have not been altered due to the presence of the transverse velocity components for the ion and electrons are given, in non-dimensional form, as follows:

ion and electron densities	$n^{\pm} = \exp\left[\pm a\,(1 - \phi)\right]$
space charge	$q = 2 \sinh\left[\, a(1 - \phi)\right]$
electric field	$E = -2\,a^{-1} \sinh\left[\frac{1}{2}\, a\,(1 - \phi)\right]$
potential	$\phi = 1 - 4\,a^{-1} \tanh^{-1}\left[\tanh\,(a/4)\, e^{-x}\right]$

sheath thickness $$\delta = \frac{1}{2} a \Big/ \sinh\left(\frac{1}{2} a\right)$$

ion current $$j_x^+ = -\left(\frac{2}{\pi m^+}\right)^{1/2} \left\{ \frac{1 - \alpha_1^+ - \beta_1^+ \operatorname{erf} c \sqrt{a}}{1 + \alpha_1^+ + \beta_1^+ \operatorname{erf} c \sqrt{a}} \right\}$$

electron current $$j_x^- = 0$$

the above sheath thickness δ is calculated from the profile of the potential. We may also define a charge thickness δ_q as,

$$\delta_q = \frac{q(0) - q(1)}{\left|\frac{dq}{dx}\right|_{\phi = 0}}$$

In the present special case, we have

$$\delta_q = (\delta \tanh a) \Big/ a$$

which indicates that this charge thickness is of the order of the sheath thickness for small a and is decreasing more rapidly than the sheath thickness as a increases.

The transverse ion velocity is now given by,

$$v^+ = V^+ \operatorname{erf} c \left[a(1 - \phi) \right]^{1/2} .$$

Together with the potential profile as illustrated in Fig. 1, we can calculate the transverse ion velocity profile and the result has been plotted in Fig. 2. The transverse ion velocity at the cathode decreases rapidly with the increase of the potential difference across the sheath. Physically, this can be traced to the trapped ions near the cathode that are originated by diffuse reflections and do not carry any transverse momentum. As the potential difference increases, more ions are trapped and the transverse ion velocity at the cathode therefore diminishes. On comparison, with the potential profile, we observe that the transverse ion velocity changes rather slowly with distance. Particularly, for large values of a, the maximum change of v^+ occurs quite a distance away from the electrode. For instance, at a distance of a Debye length from the electrode, the potential drop has reached 84% of its total value across the sheath for a = 10, but the transverse ion velocity has only reached 8% of its value at the sheath edge. Even at a distance of 5 Debye lengths, v^+/V^+ is only about 82%. This indicates that the accelerated particles begin to adjust their transverse velocities quite far away from the electrode as compared with the potential changes for high potential differences across the sheath. Further examination shows that this result is true not only for the present special case but also for the general case as can be seen from the expressions for $n^+ v^+$ and n^+ as respectively given by Eq. (9) in Section 2 and Eq. (21) in I. The transverse velocity profile of the ions is therefore an important effect to be taken into account in related practical problems.

The ion velocity slip can be calculated as

$$[V^+ - v^+(0)] / V^+ = \text{erf}(a)^{1/2}$$

which increases monotonically with a

The transverse electron velocity in the present case is given by,

$$\frac{\bar{v}}{\bar{V}} = \frac{2 - (1 - \bar{\alpha}) \text{ erf c } (a\phi)^{1/2}}{2 - (1 - \bar{\alpha}) \text{ erf c } (a)^{1/2}}$$

and the electron velocity slip is given by,

$$\frac{\bar{V} - \bar{v}(0)}{\bar{V}} = \frac{(1 - \bar{\alpha}) \text{ erf } (a)^{1/2}}{2 - (1 - \bar{\alpha}) \text{ erf c } (a)^{1/2}}$$

which also increases monotonically with a. However, as shown in Fig. 3 for $\bar{\alpha} = 0$, most of the electron velocity slip occurs near the cathode. For large a, the value of $\bar{v}/\bar{V}$ increases sharply from approximately $(1 + \bar{\alpha})/2$ to 1 in a very short distance.

Incidentally, the transverse ions and electron velocities generate a transverse current which, in turn, generates a non-uniform magnetic field near the electrode. However unless the transverse current is extremely high, the self-induced magnetic field can be neglected.

The individual pressures and temperatures of ions and electrons are given by,

$$3\bar{p}^{\pm} = 3\, n^{\pm} k\bar{T}^{\pm} = 3n^{\pm} kT - m^{\pm} n^{\pm} (u^{\pm})^2 + m^{\pm} n^{\pm} v^{\pm} (\tilde{V}^{\pm} - v^{\pm})$$

where

$$\bar{u} = 0.$$

The ion temperature for the case $\alpha_1^+ = 0$, $\beta_1^+ = 1$ and $V^+ = (kT/m^+)^{1/2}$ is plotted in Fig. 4. We note that the ion temperature, which is a weak function of the distance, is not monotonic.

The electron temperature for $V^- \sim (kT/m^-)^{-1/2}$ is almost constant throughout the sheath and rises sharply very close to the cathode.

Other quantities can be easily calculated for the special case considered here.

5. CONCLUDING REMARKS

In the present paper, we have considered the sheath structure in parallel flows by incorporating rigorously the effect of a transverse plasma velocity at the sheath edge. The results and expressions obtained here are readily applicable to related problems such as the interaction of a solid body with a moving collisionless plasma.[6] Although the interpretation of many results depends on the plasma and surface (electrode) parameters to be specified, some general conclusions can be drawn as follows:

1) The transverse velocity of accelerated particles in the sheath varies rather slowly away from the electrode in comparison with the potential. Particularly, for high potential differences across the sheath, the maximum change of the transverse velocity for the accelerated particles occurs at a distance several Debye lengths from the electrode while the maximum change of the potential always occurs at the electrode. In other words, the effect of electrode on the transverse velocity of accelerated particles may extend well beyond the distance of the sheath thickness, defined in the usual sense for high potential difference across the sheath.

2) The drag force exerted on the electrode by accelerating particles is directly proportional to the transverse velocity at the sheath edge but is independent of the potential difference across the sheath. On the other hand, the drag force due to repelled particles decreases rapidly with increasing potential differences across the sheath as one would intuitively expect.

Mathematically, the problem treated in the present paper is self-consistent and has been completely solved in terms of the electrode and plasma parameters to be specified. However, many other phases of the physical problem remain to be explored. An important one is the region outside the collisionless sheath about a mean free path away from the cathode where the neutral particles emitted from the electrode are ionized again through collisions. In this region, collisional effects and ionization effects are equally important. The kinetic model developed by the authors[7] may then provide a reasonable approach to the problem when ionization effects are included.

The most important application of the theory developed in the above is in the utilization of the results obtained for subsequent extension to the continuum domain. Except for possible numerical work, it is doubtful whether analytic results uniformly valid in the sheath and the collision domains can be obtained, because of the complexity. It is therefore suggested that the above rigorous sheath analysis can be used to provide the proper boundary conditions for a continuum approach extending beyond the sheath domain.

ACKNOWLEDGMENT

The present work was supported by the National Aeronautics and Space Administration under Contract No. NASw-1014.

REFERENCES

1. P. N. Hu and S. Ziering, Phys. Fluids, 9, 2168 - 2179 (Nov. 1966).
2. S. Aisenberg and V. Rohatgi, Appl. Phys. Letters, 8, 194 (1966).
3. E. P. Gross and S. Ziering, Phys. Fluids, 1, 215 (1958) and 2, 701 (1959).
4. S. Ziering, Phys. Fluids, 3, 503 (1960).
5. S. H. Lam and M. Greenblatt, in Rarefied Gas Dynamics (ed. by J. H. de Leeuw) Academic Press, N.Y. (1966) 2, p. 45.
6. P. N. Hu and S. Ziering, Phys. Fluids, 9, 1983 - 1988 (Oct. 1966).

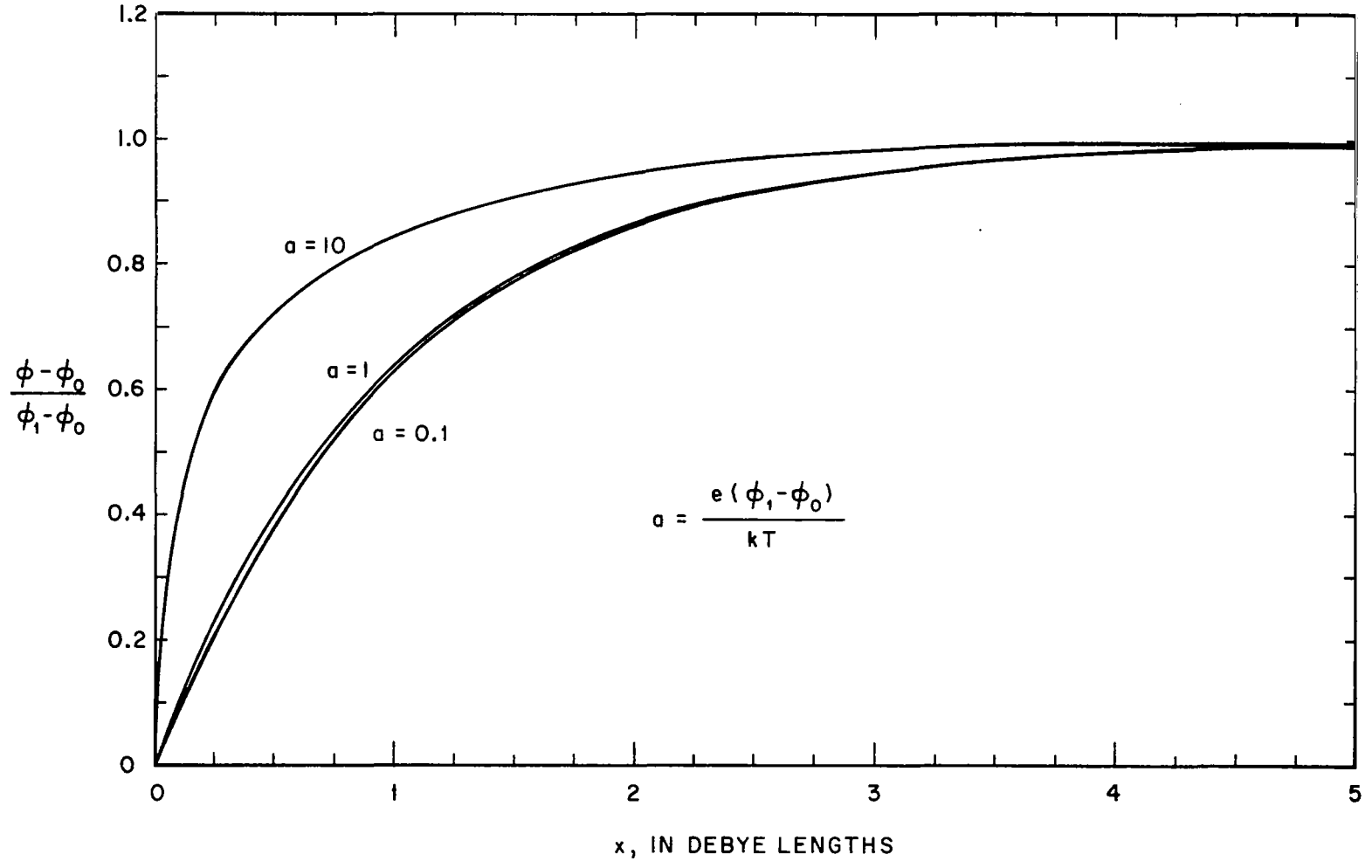

FIGURE 1.

ELECTROSTATIC POTENTIAL FOR THE CASE $\beta_0^+ = \gamma^- = E_1 = 0$, $\alpha^- + \beta^- = 1$,

$T^+ = T^- = T_0 = T$, AND $N^+ = N^- = N$.

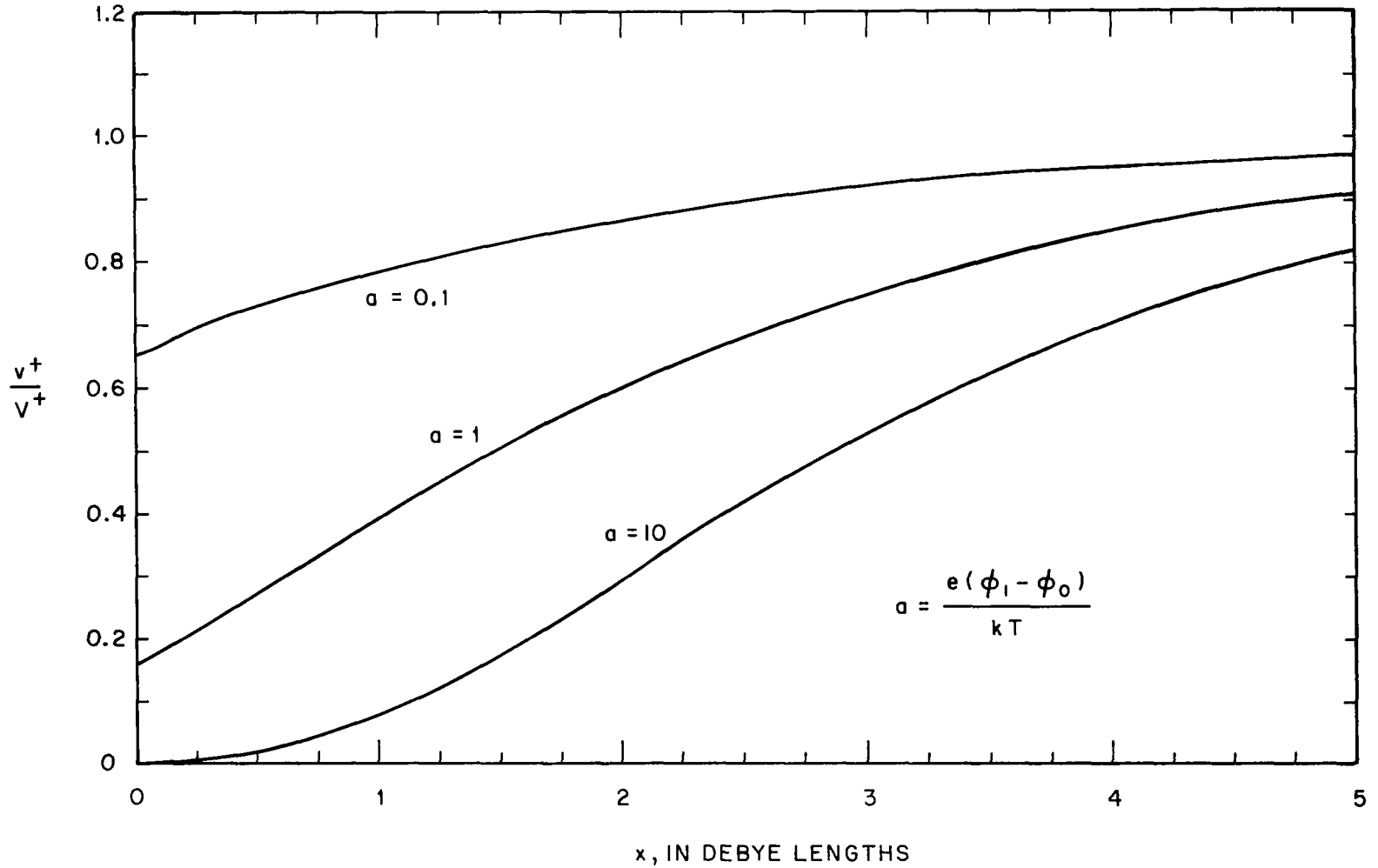

FIGURE 2.

TRANSVERSE ION VELOCITY FOR THE CASE $\beta_0^+ = \gamma^- = E_1 = 0$, $\alpha^- + \beta^- = 1$

$T^+ = T^- = T_0 = T$, AND $N^+ = N^- = N$

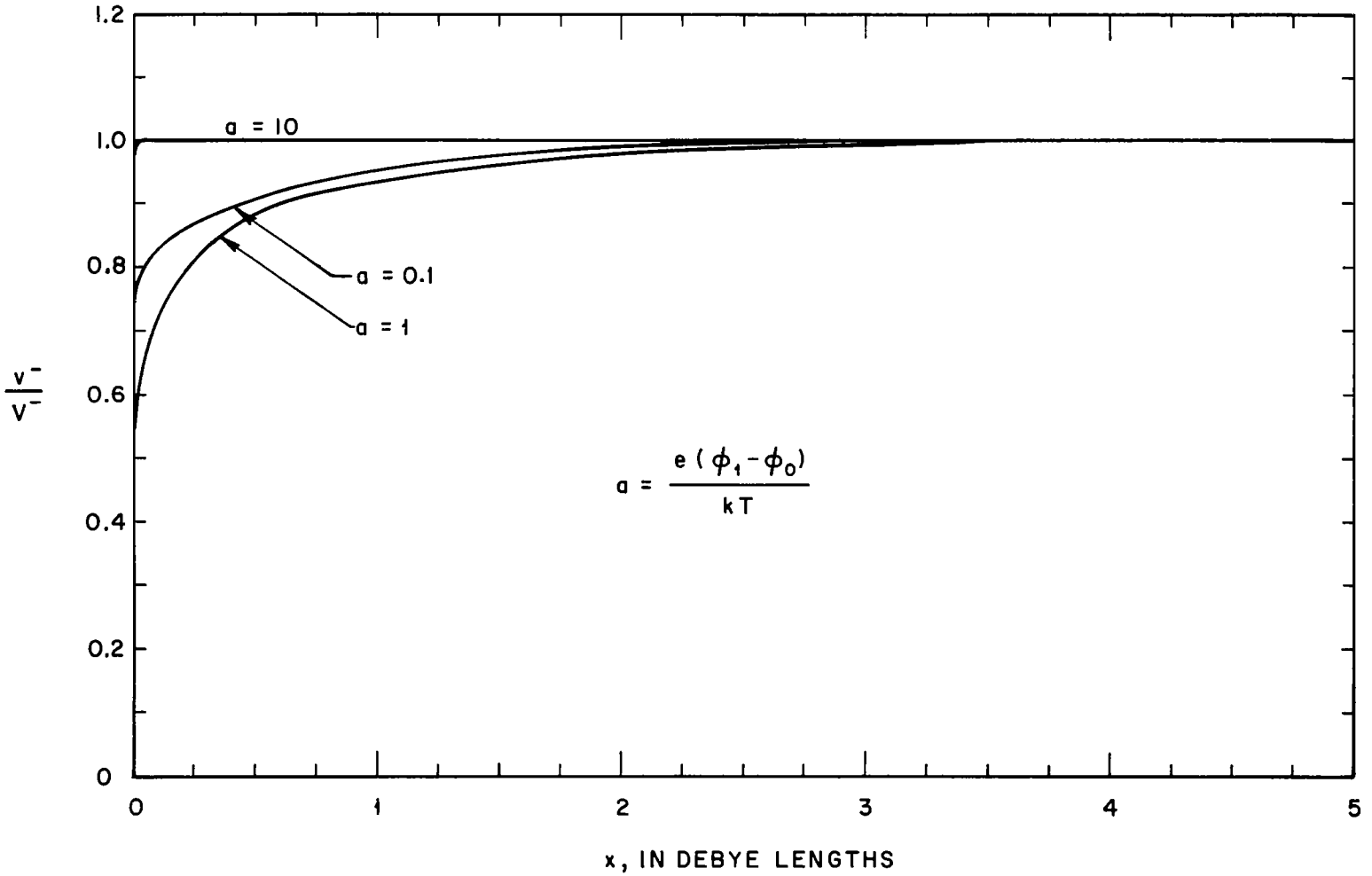

FIGURE 3.

TRANSVERSE ELECTRON VELOCITY FOR THE CASE $\beta_0^+ = \gamma^- = a^- = 0$, $\beta^- = 1$, $T^+ = T^- = T_0 = T$, AND $N^+ = N^- = N$.

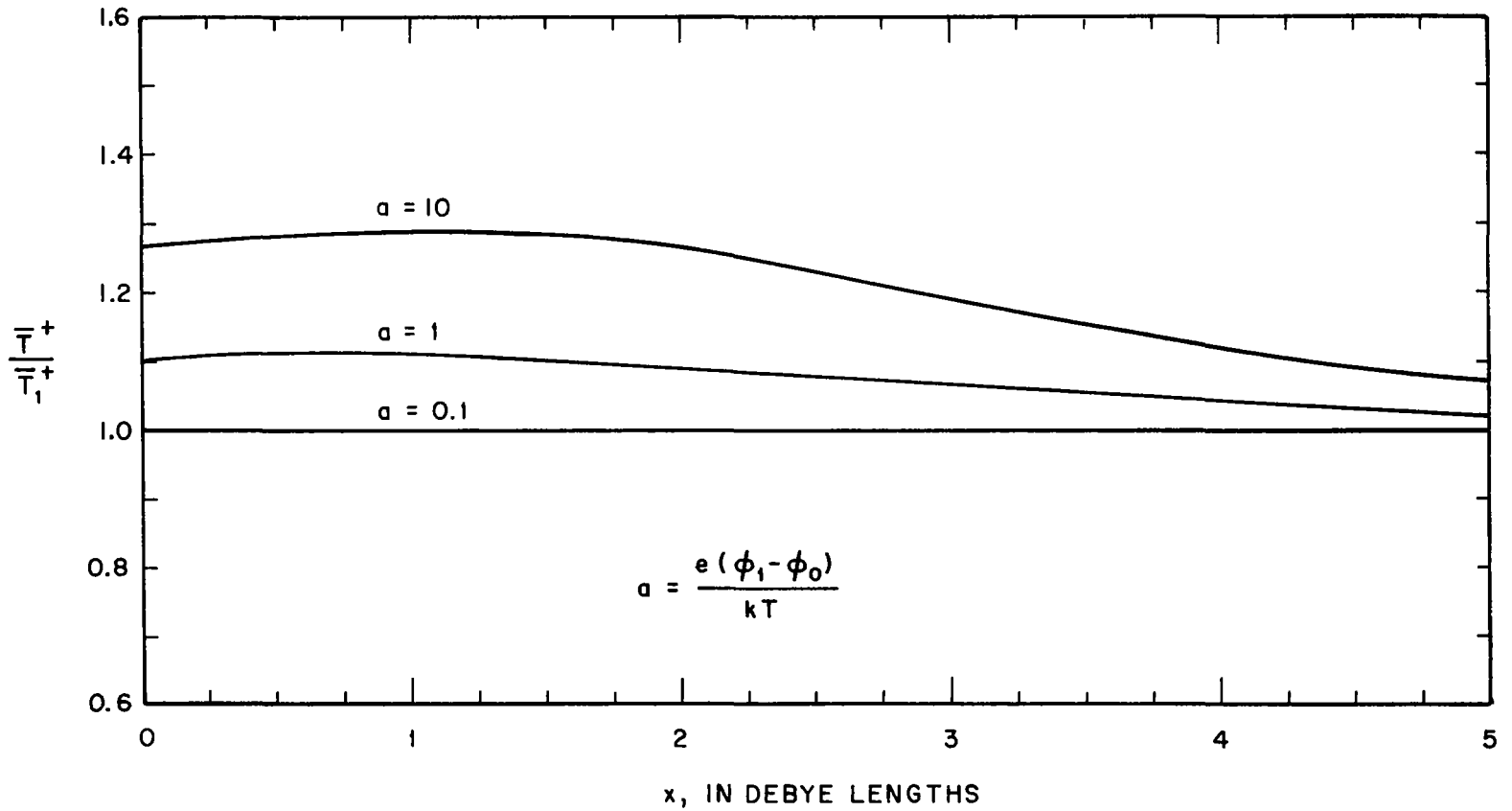

FIGURE 4.

ION TEMPERATURE FOR THE CASE $V^+ = (kT/m^+)^{\frac{1}{2}}$,

$\alpha_1^+ = \beta_0^+ = \gamma^- = E_1 = 0$, $\alpha^- + \beta^- = \beta_1^+ = 1$, $T^+ = T^- = T_0 = T$, AND $N^+ = N^- = N$.